



PUBLISHED FOR SISSA BY SPRINGER

RECEIVED: February 13, 2020

ACCEPTED: June 1, 2020

PUBLISHED: June 23, 2020

Observation of a new baryon state in the $\Lambda_b^0 \pi^+ \pi^-$ mass spectrum



The LHCb collaboration

E-mail: Ivan.Belyaev@itep.ru

ABSTRACT: A new baryon state is observed in the $\Lambda_b^0 \pi^+ \pi^-$ mass spectrum with high significance using a data sample of pp collisions, collected with the LHCb detector at centre-of-mass energies $\sqrt{s} = 7, 8$ and 13 TeV, corresponding to an integrated luminosity of 9 fb^{-1} . The mass and natural width of the new state are measured to be

$$m = 6072.3 \pm 2.9 \pm 0.6 \pm 0.2 \text{ MeV} ,$$

$$\Gamma = 72 \pm 11 \pm 2 \text{ MeV} ,$$

where the first uncertainty is statistical and the second systematic. The third uncertainty for the mass is due to imprecise knowledge of the Λ_b^0 baryon mass. The new state is consistent with the first radial excitation of the Λ_b^0 baryon, the $\Lambda_b(2S)^0$ resonance. Updated measurements of the masses and the upper limits on the natural widths of the previously observed $\Lambda_b(5912)^0$ and $\Lambda_b(5920)^0$ states are also reported.

KEYWORDS: B physics, Hadron-Hadron scattering (experiments), Heavy quark production, Spectroscopy

ARXIV EPRINT: [2002.05112](https://arxiv.org/abs/2002.05112)

Contents

1	Introduction	1
2	The LHCb detector	2
3	Event selection	3
4	Analysis of the high-mass region	5
5	Analysis of the low-mass region	9
6	Systematic uncertainties	10
7	Results and summary	14
	The LHCb collaboration	20

1 Introduction

The constituent quark model [1, 2] is very successful in describing and classifying the known hadrons based on their quantum numbers [4]. However, quantum chromodynamics that lies in the origin of the quark model, being a nonperturbative theory, does not predict hadron properties, namely masses and decay widths, from first principles. Alternative theoretical approaches are developed, such as heavy quark effective theory or lattice calculations. These approaches require verification with experiment in various regimes, *e.g.* testing the agreement with data for hadrons with different quark content and quantum numbers. Baryons, containing a beauty quark form a particular family of hadrons, where the experimental data are still scarce.

Excited beauty baryons with two light quarks and quark content bqq' , where $q, q' = u, d$, have been studied experimentally at the Tevatron and the LHC. The family of these baryons consists of the Λ_b^0 isosinglet and the Σ_b and Σ_b^* isotriplet states. The lightest charged $\Sigma_b^{(*)\pm}$ baryons have been observed by the CDF collaboration [5, 6] in the $\Lambda_b^0 \pi^\pm$ spectrum. The measurement of the masses and widths of those states was updated by the LHCb collaboration and the heavier $\Sigma_b(6097)^\pm$ states were discovered [7].

The spectrum of excited beauty baryons decaying to the $\Lambda_b^0 \pi^+ \pi^-$ final state near threshold has been studied by the LHCb collaboration using a data sample collected in 2011, which resulted in the discovery of two narrow states [8], denoted $\Lambda_b(5912)^0$ and $\Lambda_b(5920)^0$. The most likely interpretation of these states is that they are a doublet of first orbital excitations in the Λ_b^0 system, with quantum numbers $J^P = \frac{1}{2}^-$ and $\frac{3}{2}^-$, respectively. The heavier of these states was later confirmed by the CDF collaboration [9]. A doublet

Baryon	State	J^P	Ref. [16]	Ref. [17]	Ref. [18]	Ref. [19]
Λ_b^0	1S	$\frac{1}{2}^+$	5585	5612	5620	5619
	1P	$\frac{1}{2}^-$	5912	5939	5930	5911
		$\frac{3}{2}^-$	5920	5941	5942	5920
	2S	$\frac{1}{2}^+$	6045	6107	6089	
	1D	$\frac{3}{2}^+$	6145	6181	6190	6147
		$\frac{5}{2}^+$	6165	6183	6196	6153
$\Sigma_b^{(*)0}$	1S	$\frac{1}{2}^+$	5795	5833	5800	
		$\frac{3}{2}^+$	5805	5858	5834	
	1P	$\frac{1}{2}^-$	6070	6099	6101	
		$\frac{3}{2}^-$	6070	6101	6096	
		$\frac{5}{2}^-$	6090	6172	6084	
	2S	$\frac{1}{2}^+$	6200	6294	6213	
		$\frac{3}{2}^+$	6250	6308	6226	

Table 1. Quark-model predictions for the masses of the lightest Λ_b and $\Sigma_b^{(*)}$ states (in MeV).

of narrow states, $\Lambda_b(6146)^0$ and $\Lambda_b(6152)^0$, was also observed by LHCb collaboration [10]. The measured masses and widths of these states are compatible with the expectations for the $\Lambda_b(1D)^0$ doublet [11–14]. Recently, the CMS collaboration reported an evidence for a broad excess of events in the $\Lambda_b^0\pi^+\pi^-$ mass spectrum in the region of 6040 – 6100 MeV corresponding to a statistical significance of four standard deviations [15].¹ The existence of additional states in the $\Lambda_b^0\pi^+\pi^-$ spectrum is predicted by the quark model [16–18], notably, in the region between the established narrow doublet states, with masses around 6.1 GeV. Quark-model predictions for the masses of the lightest Λ_b and $\Sigma_b^{(*)}$ states are shown in table 1.

This paper reports the observation of a new structure in the $\Lambda_b^0\pi^+\pi^-$ mass spectrum, as well as updated measurements of the masses and widths of the $\Lambda_b(5912)^0$ and $\Lambda_b(5920)^0$ states with improved precision. The analysis uses pp collision data recorded by LHCb in 2011–2018 at centre-of-mass energies of 7, 8 and 13 TeV, corresponding to an integrated luminosity of 1, 2 and 6 fb^{−1}, respectively.

2 The LHCb detector

The LHCb detector [20, 21] is a single-arm forward spectrometer covering the pseudo-rapidity range $2 < \eta < 5$, designed for the study of particles containing b or c quarks.

¹Natural units are used through the paper with $c = \hbar = 1$.

The detector includes a high-precision tracking system consisting of a silicon-strip vertex detector surrounding the pp interaction region [22], a large-area silicon-strip detector located upstream of a dipole magnet with a bending power of about 4 Tm, and three stations of silicon-strip detectors and straw drift tubes [23, 24] placed downstream of the magnet. The tracking system provides a measurement of the momentum, p , of charged particles with a relative uncertainty that varies from 0.5% at low momentum to 1.0% at 200 GeV. The momentum scale of the tracking system is calibrated using samples of $J/\psi \rightarrow \mu^+\mu^-$ and $B^+ \rightarrow J/\psi K^+$ decays collected concurrently with the data sample used for this analysis [25, 26]. The relative accuracy of this procedure is estimated to be 3×10^{-4} using samples of other fully reconstructed b-hadron, K_S^0 , and narrow $\Upsilon(1S)$ resonance decays. Different types of charged hadrons are distinguished by the particle identification (PID) system using information from two ring-imaging Cherenkov detectors [27]. Muons are identified by a system composed of alternating layers of iron and multiwire proportional chambers [28].

The online event selection is performed by a trigger [29] which consists of a hardware stage, based on information from the calorimeter and muon systems, followed by a software stage, which applies a full event reconstruction. At the hardware trigger stage, events are required to have a muon with high transverse momentum, p_T , or a pair of opposite-sign muons with a requirement on the product of muon transverse momenta, or a hadron, photon or electron with high transverse energy in the calorimeters. The software trigger requires a two-, three- or four-track secondary vertex with at least one charged particle with a large p_T and inconsistent with originating from any reconstructed primary pp collision vertex (PV) [30, 31] or two muons of opposite charge forming a good-quality secondary vertex with a mass in excess of 2.7 GeV.

Simulation is required to model the effects of the detector acceptance, resolution, and selection requirements. In the simulation, pp collisions are generated using PYTHIA [32] with a specific LHCb configuration [33]. Decays of unstable particles are described by EVTGEN [34], in which final-state radiation is generated using PHOTOS [35]. The interaction of the generated particles with the detector, and its response, are implemented using the GEANT4 toolkit [36] as described in ref. [38].

3 Event selection

The Λ_b^0 candidates are reconstructed in the $\Lambda_b^0 \rightarrow \Lambda_c^+ \pi^-$ and the $\Lambda_b^0 \rightarrow J/\psi p K^-$ decays.² The selection of the Λ_b^0 candidates is similar to that used in ref. [10]. All charged final-state particles are required to be positively identified by the PID systems. To reduce the background from random combinations of tracks, only the tracks with large impact parameter with respect to all PVs in the event are used. The Λ_c^+ candidates are reconstructed in the $p K^- \pi^+$ final state. The $\Lambda_b^0 \rightarrow J/\psi p K^-$ candidates are created by combining the J/ψ candidates formed of $\mu^+\mu^-$ pairs with kaon and proton tracks. The masses of the Λ_c^+ and J/ψ candidates are required to be consistent with the known values of the masses

²Inclusion of charge-conjugate states is implied throughout this paper.

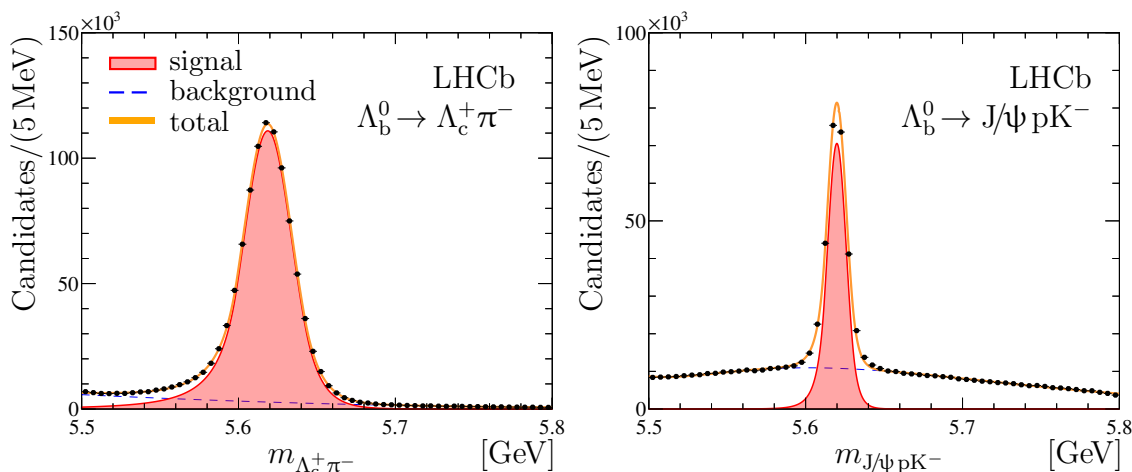


Figure 1. Mass distributions for selected (left) $\Lambda_b^0 \rightarrow \Lambda_c^+ \pi^-$ and (right) $\Lambda_b^0 \rightarrow J/\psi p K^-$ candidates after BDT selection. A fit, composed of a sum of a double-sided Crystal Ball function [46] and a smooth background component, is overlaid.

of the respective states [4] and the Λ_b^0 candidate is required to have a good-quality vertex significantly displaced from all PVs.

Further suppression of the background is achieved by using a boosted decision tree (BDT) classifier [39, 40] implemented in the TMVA toolkit [41]. Two separate BDTs are used for the $\Lambda_b^0 \rightarrow \Lambda_c^+ \pi^-$ and $\Lambda_b^0 \rightarrow J/\psi p K^-$ selections. The multivariate estimators are based on the kinematic properties, the reconstructed lifetime and vertex quality of the Λ_b^0 candidate and on variables describing the overall consistency of the selected candidates with the decay chain obtained from the kinematic fit described below [43]. In addition, the reconstructed lifetime and vertex quality of the $\Lambda_c^+ \rightarrow p K^- \pi^+$ candidate is used for the $\Lambda_b^0 \rightarrow \Lambda_c^+ \pi^-$ decay. The PID quality, transverse momentum and pseudorapidity of the proton and kaon candidates (for $\Lambda_b^0 \rightarrow J/\psi p K^-$) or π^- candidate (for $\Lambda_b^0 \rightarrow \Lambda_c^+ \pi^-$) are also used. The BDT is trained using data, where the signal sample is obtained by subtracting the background using the *sPlot* technique [44], and the background sample is taken from the range 5.70 – 5.85 GeV in the $\Lambda_b^0 \rightarrow \Lambda_c^+ \pi^-$ and $\Lambda_b^0 \rightarrow J/\psi p K^-$ mass distributions. A *k*-fold cross-validation technique is used to avoid introducing a bias in the evaluation [45]. A kinematic fit [43] is performed in order to improve the Λ_b^0 mass resolution. The momenta of the particles in the full decay chain are recomputed by constraining the Λ_c^+ or J/ψ mass to their known values [4] and the Λ_b^0 baryon to originate from the associated PV. The mass distributions for the selected $\Lambda_b^0 \rightarrow \Lambda_c^+ \pi^-$ and $\Lambda_b^0 \rightarrow J/\psi p K^-$ candidates are shown in figure 1. The Λ_b^0 signal yield is $(937.9 \pm 1.6) \times 10^3$ and $(223.0 \pm 0.6) \times 10^3$ for $\Lambda_b^0 \rightarrow \Lambda_c^+ \pi^-$ and $\Lambda_b^0 \rightarrow J/\psi p K^-$ decays, respectively.

Selected $\Lambda_b^0 \rightarrow \Lambda_c^+ \pi^-$ ($\Lambda_b^0 \rightarrow J/\psi p K^-$) candidates with mass within ± 50 (20) MeV from the known Λ_b^0 mass are combined with pairs of opposite and same-sign pion tracks. To reduce the large combinatorial background, four separate BDT classifiers are trained for the $\Lambda_b^0 \rightarrow \Lambda_c^+ \pi^-$ and $\Lambda_b^0 \rightarrow J/\psi p K^-$ samples in the high-mass ($m_{\Lambda_b^0 \pi\pi} < 6.35$ GeV) and the low-mass ($m_{\Lambda_b^0 \pi\pi} < 5.95$ GeV) regions. The BDTs exploit the vertex quality, χ_{vtx}^2 , of

the $\Lambda_b^0 \pi \pi$ combination, its transverse momentum, the p_T of the $\pi \pi$ pair, the p_T of each pion, as well as their PID and track-reconstruction-quality variables. For the high-mass region, the p_T of the dipion system is required to exceed 250 MeV. Simulated samples of excited Λ_b^0 baryons decaying into the $\Lambda_b^0 \pi^+ \pi^-$ final state are used as signal training samples, while the background training sample is taken from the same-sign $\Lambda_b^0 \pi^\pm \pi^\pm$ combinations in data. For the low-mass region, simulated samples of $\Lambda_b(5912)^0$ and $\Lambda_b(5920)^0$ signal decays are used, while for the high-mass region the simulated sample consists of decays of a narrow state with mass of 6.15 GeV and natural width of 7 MeV, and a broad state with mass of 6.08 GeV and natural width of 60 MeV. A k -fold cross-validation technique is used for training. A figure of merit $\varepsilon/(\frac{5}{2} + \sqrt{B})$ [47] is used to optimise the requirement on the BDT estimator. The $\Lambda_b^0 \pi \pi$ mass resolution is improved by a kinematic fit [43] constraining the mass of the $pK^- \pi^+$ and $\mu^+ \mu^-$ combinations to the known masses of the Λ_c^+ baryon and J/ψ meson, respectively [4]. The mass of the Λ_b^0 baryon in the fit is constrained to the central value of $m_{\Lambda_b^0} = 5619.62 \pm 0.16 \pm 0.13$ MeV [48]. It is also required that the momentum vector of the Λ_b^0 candidate and the momenta of both pions points back to the associated pp interaction vertex.

4 Analysis of the high-mass region

The distributions of the $\Lambda_b^0 \pi^+ \pi^-$ and $\Lambda_b^0 \pi^\pm \pi^\pm$ masses in the range $5.93 < m_{\Lambda_b^0 \pi \pi} < 6.23$ GeV for the $\Lambda_b^0 \rightarrow \Lambda_c^+ \pi^-$ sample with the high-mass BDT selection applied are shown in figure 2. The distributions of the same-sign $\Lambda_b^0 \pi^\pm \pi^\pm$ combinations are dominated by random combinations of a Λ_b^0 baryon and two pions. The $\Lambda_b^0 \pi^+ \pi^-$ spectrum features the contributions of two narrow $\Lambda_b(6146)^0$ and $\Lambda_b(6152)^0$ states as well as a broad structure just below 6.1 GeV in addition to the smooth background. This new structure is referred to as Λ_b^{*0} hereafter. Figure 3 shows the same distributions for the $\Lambda_b^0 \rightarrow J/\psi pK^-$ sample, where the same features are visible.

A simultaneous binned maximum-likelihood fit with a bin width of 200 keV is performed to the six distributions shown in figures 2 and 3 in order to determine the properties of the resonant shapes. Both signal and background $\Lambda_b^0 \pi \pi$ combinations could include contributions from intermediate Σ_b^\pm and $\Sigma_b^{*\pm}$ states. The fitting function for the $\Lambda_b^0 \pi^+ \pi^-$ spectra is the sum of five components: a combinatorial background, the two components corresponding to the combinations of $\Sigma_b^\pm \rightarrow \Lambda_b^0 \pi^\pm$ and $\Sigma_b^{*\pm} \rightarrow \Lambda_b^0 \pi^\pm$ with the addition of a pion from the rest of the event, and three resonant contributions for the $\Lambda_b(6146)^0$, $\Lambda_b(6152)^0$ and Λ_b^{*0} states. The same-sign $\Lambda_b^0 \pi^\pm \pi^\pm$ spectra are fitted with a function that contains only the combinatorial, $\Sigma_b^\pm \pi^\pm$, and $\Sigma_b^{*\pm} \pi^\pm$ components.

The combinatorial background is parameterised with a positive, increasing third-order polynomial function, whose coefficients are left free to vary in the fit. The $\Sigma_b^\pm \pi$ and $\Sigma_b^{*\pm} \pi$ components are described by the product of a two-body phase-space function and an exponential function, accounting for the finite width of the $\Sigma_b^{(*)}$ states. The exponential factor is determined from the fit to the background-subtracted $\Sigma_b^{(*)\pm} \pi$ mass distributions in the $6.16 < m_{\Lambda_b^0 \pi \pi} < 6.40$ GeV range. The shapes of the $\Sigma_b^{(*)\pm} \pi$ components are taken to be the same in all spectra. The combinatorial background shape is fixed to be the same

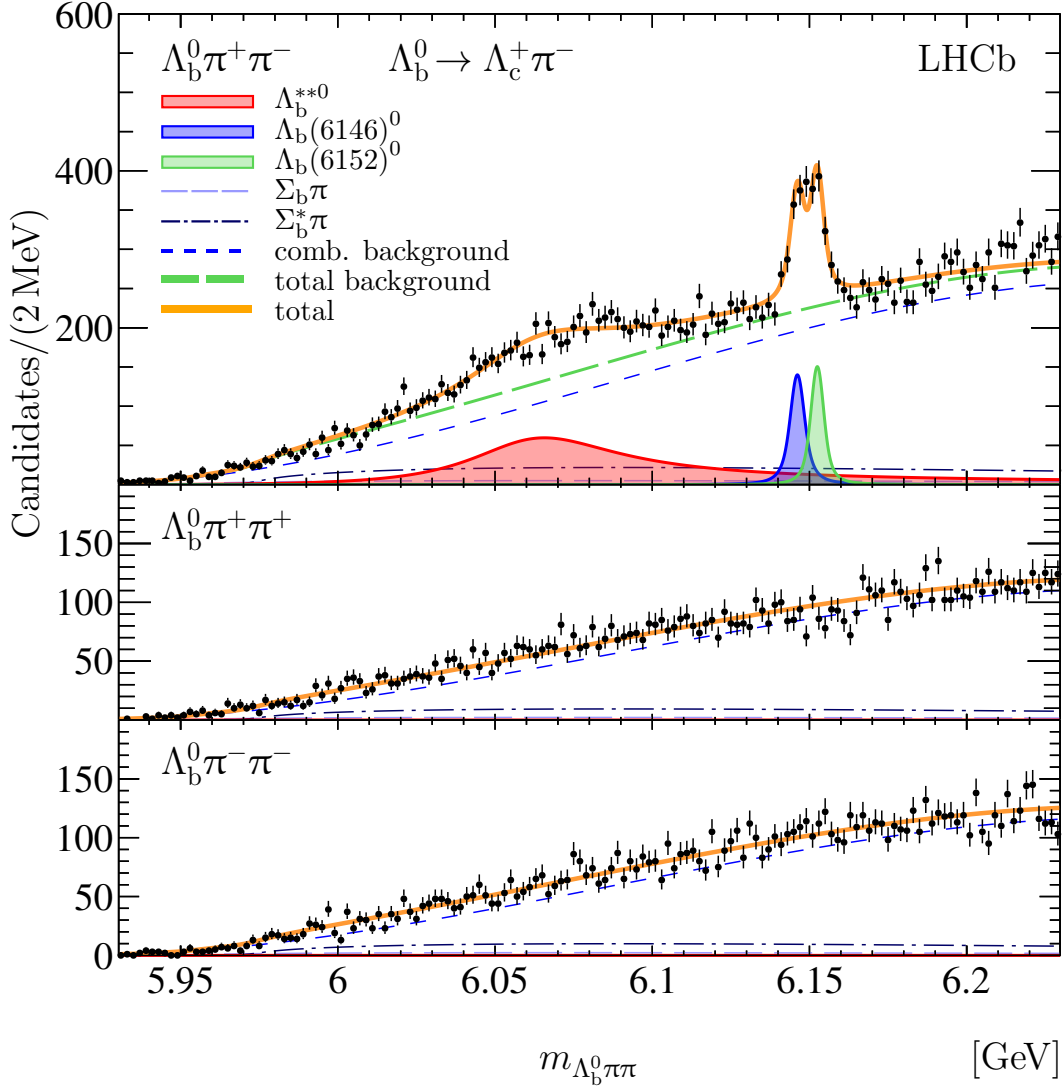


Figure 2. Mass spectra of selected (top) $\Lambda_b^0 \pi^+ \pi^-$, (middle) $\Lambda_b^0 \pi^+ \pi^+$ and (bottom) $\Lambda_b^0 \pi^- \pi^-$ combinations for the $\Lambda_b^0 \rightarrow \Lambda_c^+ \pi^-$ sample. A simultaneous fit, described in the text, is superimposed.

in the opposite-sign $\Lambda_b^0 \pi^+ \pi^-$ and same-sign $\Lambda_b^0 \pi^\pm \pi^\pm$ spectra, but is allowed to differ for the $\Lambda_b^0 \rightarrow \Lambda_c^+ \pi^-$ and $\Lambda_b^0 \rightarrow J/\psi p K^-$ samples. The yields of all background components are left free to vary in the fit. A good description of both the $\Lambda_b^0 \pi^+ \pi^+$ and $\Lambda_b^0 \pi^- \pi^-$ mass spectra supports the chosen background model.

The narrow $\Lambda_b(6146)^0$ and $\Lambda_b(6152)^0$ components are parameterised using relativistic Breit-Wigner distributions convolved with the experimental resolution. The detector resolution function is described by the sum of two Gaussian functions with zero mean and parameters fixed from simulation. The obtained effective resolution increases from 0.5 MeV to 1.7 MeV when the $\Lambda_b^0 \pi^+ \pi^-$ mass grows from the mass of the $\Lambda_b(5912)^0$ state to that of the $\Lambda_b(6152)^0$ state. The masses and widths of the $\Lambda_b(6146)^0$ and $\Lambda_b(6152)^0$ states are fixed to the values obtained in ref. [10]. The Λ_b^{*0} shape as a function of the $\Lambda_b^0 \pi \pi$ mass m

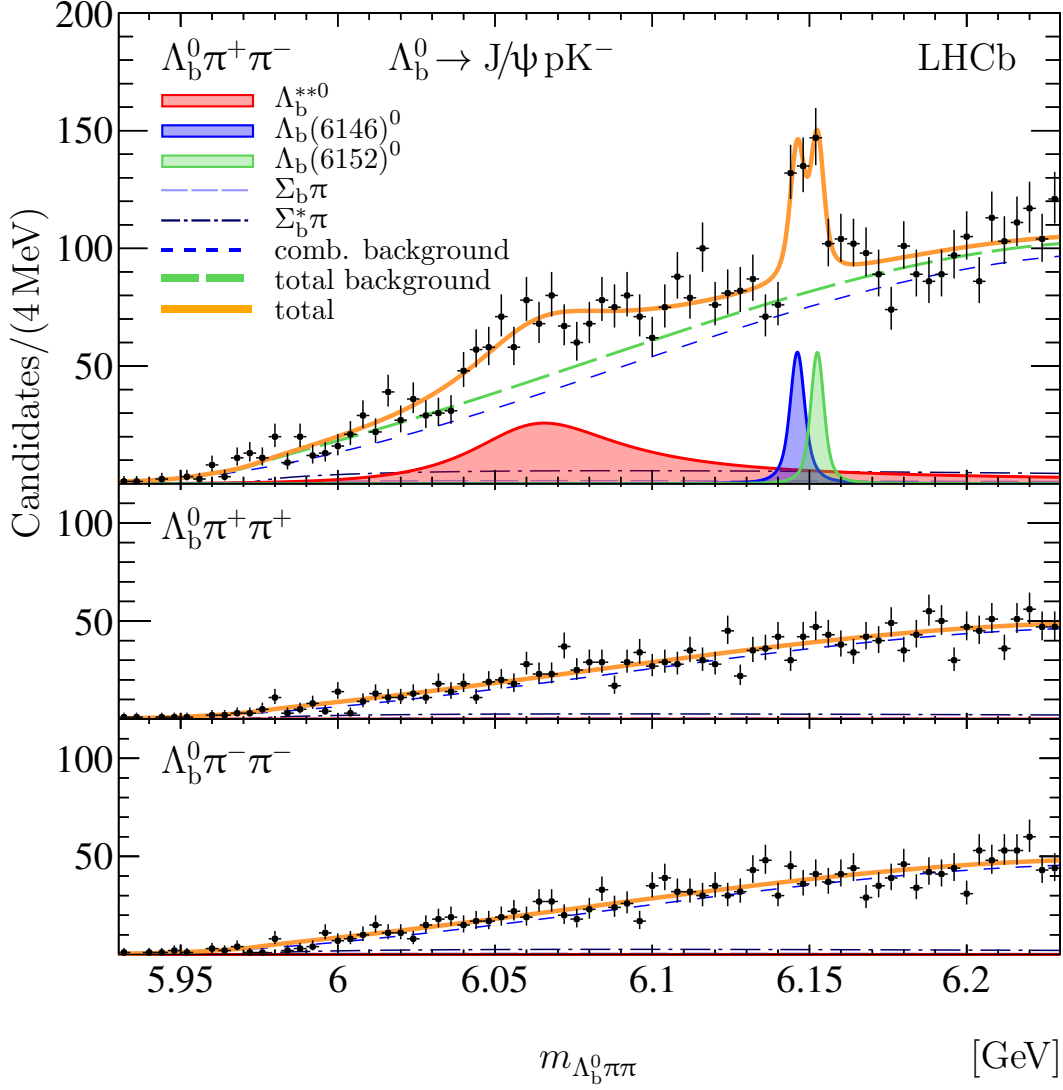


Figure 3. Mass spectra of selected (top) $\Lambda_b^0 \pi^+ \pi^-$, (middle) $\Lambda_b^0 \pi^+ \pi^+$ and (bottom) $\Lambda_b^0 \pi^- \pi^-$ combinations for the $\Lambda_b^0 \rightarrow J/\psi p K^-$ sample. A simultaneous fit, described in the text, is superimposed.

is parameterised as

$$\mathfrak{S}(m|m_0, \Gamma) \propto \frac{\Gamma \rho_3(m)}{(m_0^2 - m^2)^2 + m_0^2 \Gamma^2 \left(\frac{\rho_3(m)}{\rho_3(m_0)} \right)^2}, \quad (4.1)$$

where $\rho_3(m)$ is a three-body phase space of the $\Lambda_b^0 \pi^+ \pi^-$ system

$$\rho_3(m) \equiv \frac{\pi^2}{4m^2} \int_{4m_\pi^2}^{(m-m_{\Lambda_b^0})^2} \frac{dm_{\pi\pi}^2}{m_{\pi\pi}^2} \lambda^{1/2}(m_{\pi\pi}^2, m^2, m_{\Lambda_b^0}^2) \lambda^{1/2}(m_{\pi\pi}^2, m_\pi^2, m_\pi^2), \quad (4.2)$$

$\lambda(x, y, z)$ stands for a Källén function [49], and m_π and $m_{\Lambda_b^0}$ denote the known masses

	$\Lambda_b^0 \rightarrow \Lambda_c^+ \pi^-$	$\Lambda_b^0 \rightarrow J/\psi p K^-$
Λ_b^{**0}	2570 ± 260	550 ± 80
$\Lambda_b(6146)^0$	520 ± 50	103 ± 22
$\Lambda_b(6152)^0$	480 ± 50	90 ± 21

Table 2. Yields of excited baryons from the simultaneous fit to $\Lambda_b^0 \pi \pi$ spectra with $\Lambda_b^0 \rightarrow \Lambda_c^+ \pi^-$ and $\Lambda_b^0 \rightarrow J/\psi p K^-$.

of the charged π meson and Λ_b^0 baryon, respectively. The mass, m_0 , and width, Γ , of the Λ_b^{**0} state are free parameters of the fit.

The yields of the fit components in the combined fit are reported in table 2. The mass difference with respect to the Λ_b^0 baryon mass and the natural width of the Λ_b^{**0} state are determined to be

$$\begin{aligned}\Delta m_{\Lambda_b^{**0}} &= 452.7 \pm 2.9 \text{ MeV}, \\ \Gamma_{\Lambda_b^{**}} &= 72 \pm 11 \text{ MeV},\end{aligned}$$

where uncertainties are statistical only. The statistical significance of the Λ_b^{**0} signal in $\Lambda_b^0 \rightarrow \Lambda_c^+ \pi^-$ and $\Lambda_b^0 \rightarrow J/\psi p K^-$ samples is obtained using Wilks' theorem [50] and exceeds 14 and 7 standard deviations, respectively. The ratios of the Λ_b^{**0} , $\Lambda_b(6146)^0$ and $\Lambda_b(6152)^0$ signal yields between the $\Lambda_b^0 \rightarrow \Lambda_c^+ \pi^-$ and $\Lambda_b^0 \rightarrow J/\psi p K^-$ final state are larger than the ratio of their yields reported in section 3. This arises due to the difference in the p_T spectra selected by the trigger for these final states which is propagated to the $\pi\pi$ reconstruction effects.

The earlier analysis of $\Lambda_b(6146)^0$ and $\Lambda_b(6152)^0$ states [10] has shown that a significant fraction of their decays into the $\Lambda_b^0 \pi^+ \pi^-$ final state proceeds via the intermediate $\Sigma_b^\pm \pi^\mp$ and $\Sigma_b^{*\pm} \pi^\mp$ processes. Since the measured mass of the Λ_b^{**0} state is above the $\Sigma_b \pi$ threshold, one might expect that this state decays via intermediate $\Sigma_b^{(*)\pm} \pi^\mp$ states as well. However, performing the fits to the $\Sigma_b^{(*)} \pi$ mass spectra as was done in ref. [10] is complicated by the fact that the $\Sigma_b^{(*)\pm} \pi^\mp$ and $\Sigma_b^{(*)\mp} \pi^\pm$ kinematic regions overlap in the range of $\Lambda_b^0 \pi^+ \pi^-$ masses used for the Λ_b^{**0} fit. Separating the contributions of the resonant and nonresonant Λ_b^{**0} decays would require a full multidimensional fit in the $\Lambda_b^0 \pi^+ \pi^-$, $\Lambda_b^0 \pi^+$ and $\Lambda_b^0 \pi^-$ masses, which is beyond the scope of this paper.

The $\Lambda_b^0 \pi^\pm$ mass spectra from $\Lambda_b^0 \pi^+ \pi^-$ and $\Lambda_b^0 \pi^\pm \pi^\pm$ combinations with $\Lambda_b^0 \rightarrow \Lambda_c^+ \pi^-$ from the Λ_b^{**0} signal-enhanced region $6.00 < m_{\Lambda_b^0 \pi \pi} < 6.14 \text{ GeV}$ are shown in figure 4. The $\Lambda_b^0 \pi^\pm$ mass spectrum from the signal Λ_b^{**0} decays is obtained assuming that the $\Lambda_b^0 \pi^\pm$ spectra from the same-sign $\Lambda_b^0 \pi^\pm \pi^\pm$ combinations represent the background. The background-subtracted spectrum is consistent with the presence of relatively small contributions from $\Lambda_b^{**0} \rightarrow \Sigma_b^\pm \pi^\mp$ and $\Lambda_b^{**0} \rightarrow \Sigma_b^{*\pm} \pi^\mp$ decays and a dominant contribution from nonresonant $\Lambda_b^{**0} \rightarrow \Lambda_b^0 \pi^+ \pi^-$ decays.

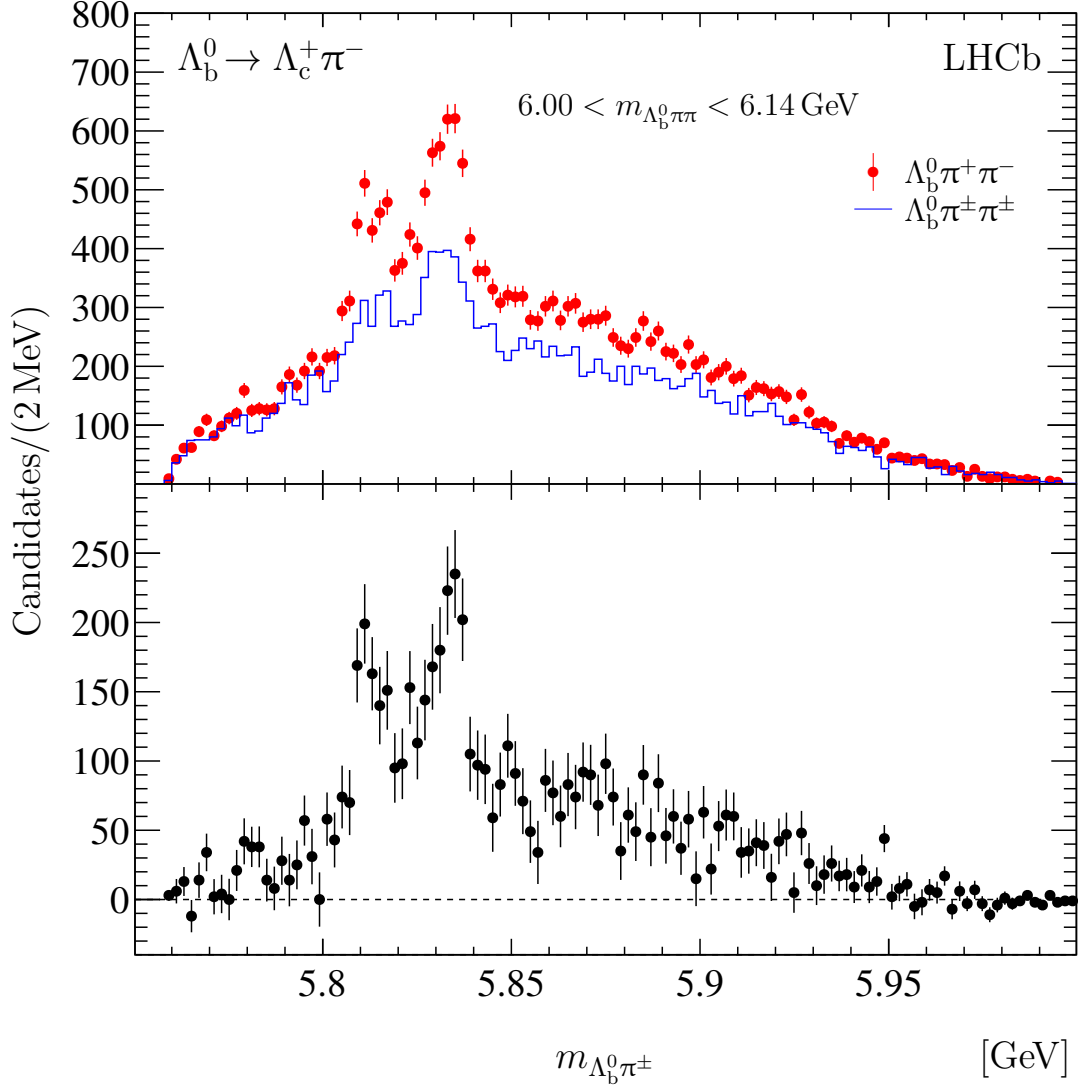


Figure 4. (Top) Spectra of $\Lambda_b^0 \pi^\pm$ mass with $\Lambda_b^0 \rightarrow \Lambda_c^+ \pi^-$ for $\Lambda_b^0 \pi^+ \pi^-$ combinations (red points with error bars) and $\Lambda_b^0 \pi^\pm \pi^\pm$ combinations (open blue histogram). (Bottom) Difference between $\Lambda_b^0 \pi$ mass spectra from $\Lambda_b^0 \pi^+ \pi^-$ and $\Lambda_b^0 \pi^\pm \pi^\pm$ combinations. The structures near 5.81 and 5.83 GeV correspond to the $\Sigma_b^\pm \rightarrow \Lambda_b^0 \pi^\pm$ and $\Sigma_b^{*\pm} \rightarrow \Lambda_b^0 \pi^\pm$ signals, respectively.

5 Analysis of the low-mass region

The $\Lambda_b^0 \pi \pi$ mass spectra in the low-mass region $m_{\Lambda_b^0 \pi \pi} < 5.94 \text{ GeV}$ for $\Lambda_b^0 \rightarrow \Lambda_c^+ \pi^-$ and $\Lambda_b^0 \rightarrow J/\psi p K^-$ samples are shown in figures 5 and 6, respectively. These distributions are used to measure the properties of the $\Lambda_b(5912)^0$ and $\Lambda_b(5920)^0$ states. A simultaneous binned fit, with narrow bins of 50 keV width, is performed to the six distributions with the sum of the two resonance components (in $\Lambda_b^0 \pi^+ \pi^-$ combinations only) and the combinatorial background component (in all six distributions). The combinatorial component is parameterised with a product of the three-body phase-space function and a positive polynomial function. The resonant components are given by relativistic S -wave Breit-Wigner

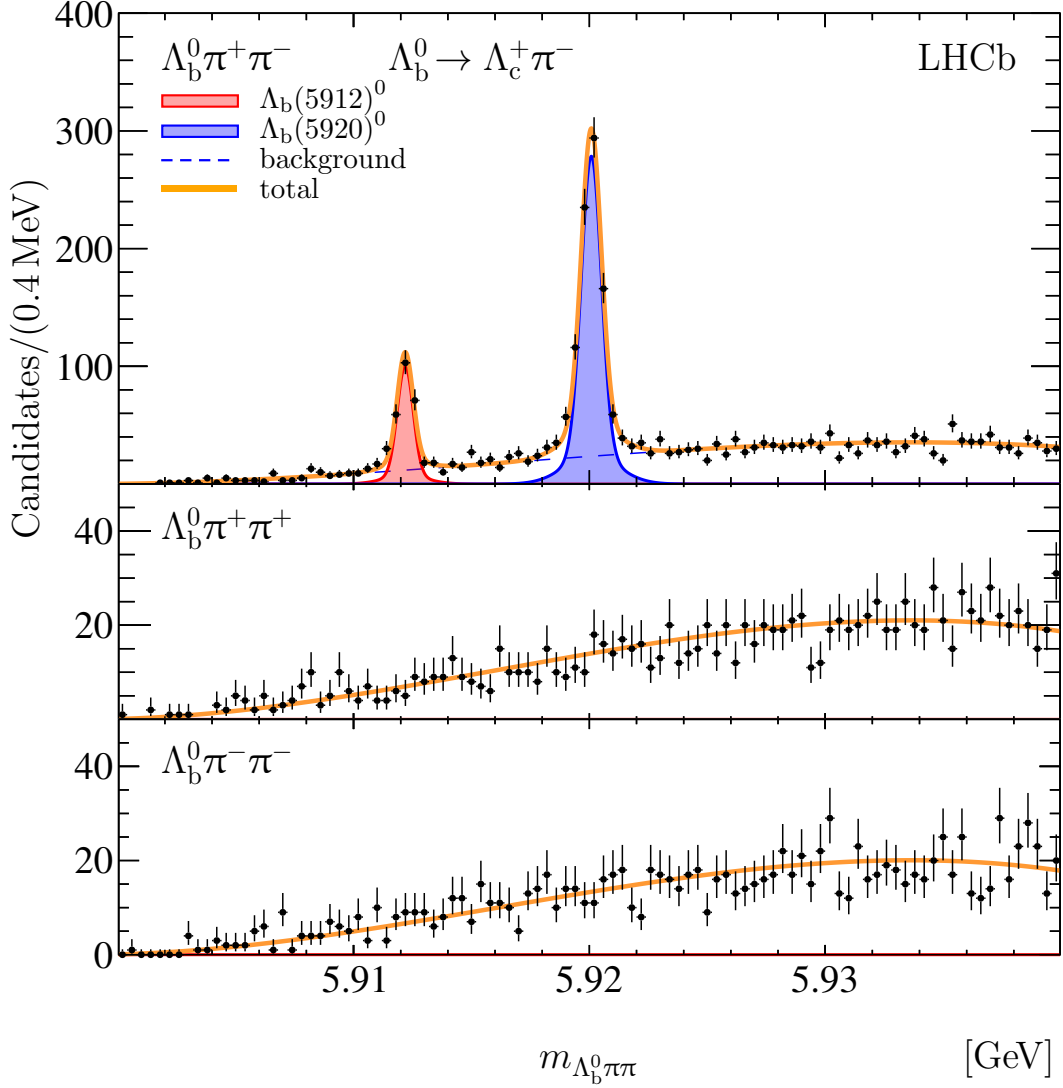


Figure 5. Mass spectra of selected (top) $\Lambda_b^0 \pi^+ \pi^-$, (middle) $\Lambda_b^0 \pi^+ \pi^+$ and (bottom) $\Lambda_b^0 \pi^- \pi^-$ combinations for the $\Lambda_b^0 \rightarrow \Lambda_c^+ \pi^-$ sample. A simultaneous fit, described in the text, is superimposed.

lineshapes convolved with the resolution function obtained from simulation. The shape of the combinatorial background is assumed to be the same in the opposite-sign $\Lambda_b^0 \pi^+ \pi^-$ and same-sign $\Lambda_b^0 \pi^\pm \pi^\pm$ spectra, but is allowed to differ for the $\Lambda_b^0 \rightarrow \Lambda_c^+ \pi^-$ and $\Lambda_b^0 \rightarrow J/\psi p K^-$ samples. The results of the combined fit are presented in table 3. The natural widths of the $\Lambda_b(5912)^0$ and $\Lambda_b(5920)^0$ states are consistent with zero.

6 Systematic uncertainties

The systematic uncertainties of the mass and the width of the Λ_b^{*0} state and of the masses of the $\Lambda_b(5912)^0$ and $\Lambda_b(5920)^0$ states are summarised in table 4.

A large uncertainty in the measurement of the Λ_b^{*0} parameters comes from the parameterisation of the Λ_b^{*0} signal distribution. The fit function from eq. (4.1) describes

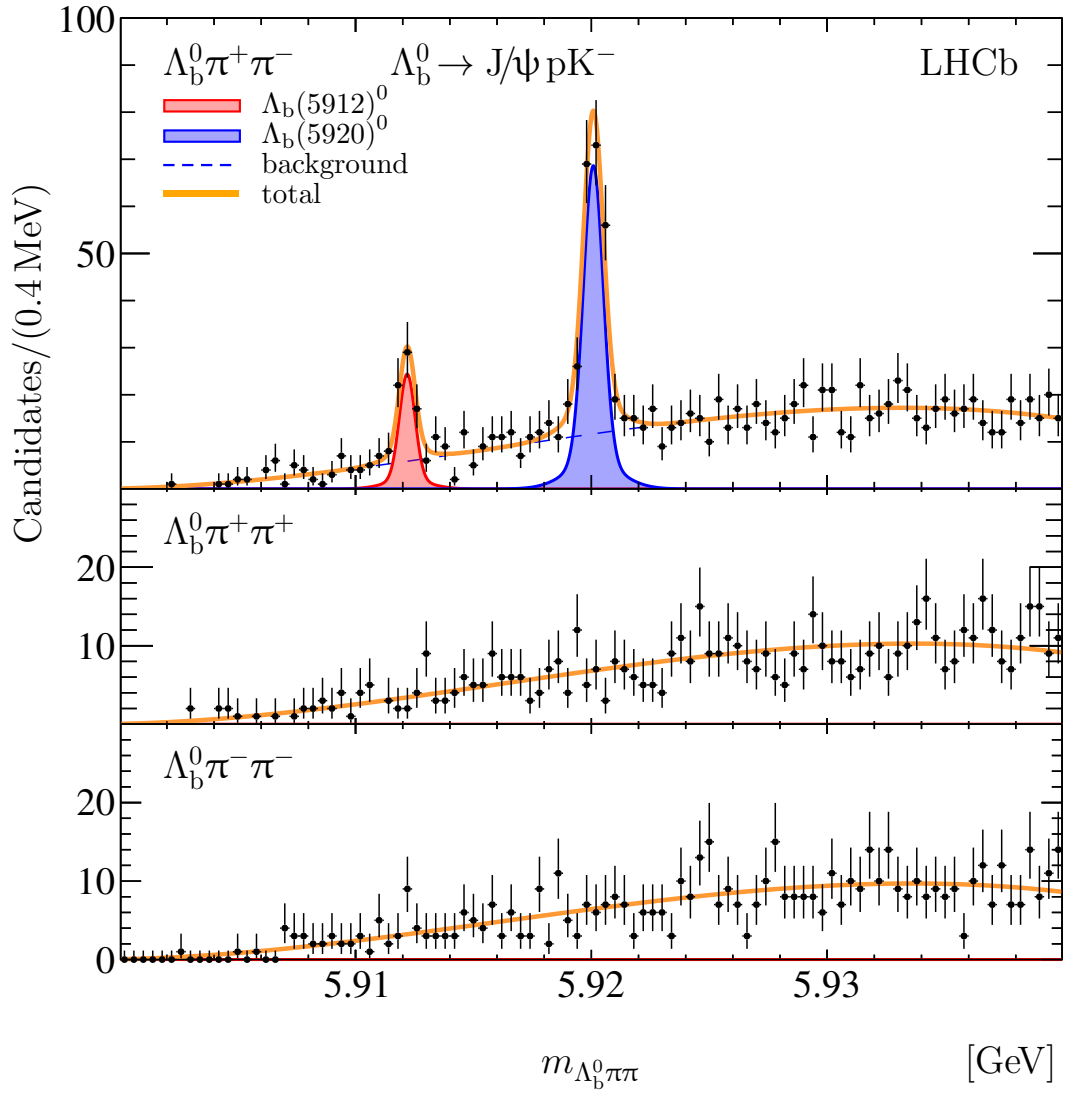


Figure 6. Mass spectra of selected (top) $\Lambda_b^0 \pi^+ \pi^-$, (middle) $\Lambda_b^0 \pi^+ \pi^+$ and (bottom) $\Lambda_b^0 \pi^- \pi^-$ combinations for the $\Lambda_b^0 \rightarrow J/\psi p K^-$ sample. A simultaneous fit, described in the text, is superimposed.

	$\Lambda_b^0 \rightarrow \Lambda_c^+ \pi^-$	$\Lambda_b^0 \rightarrow J/\psi p K^-$
$N_{\Lambda_b(5912)^0}$	234 ± 17	57 ± 9
$N_{\Lambda_b(5920)^0}$	843 ± 33	204 ± 17
$\Delta m_{\Lambda_b(5912)^0}$ [MeV]	292.582 ± 0.029	
$\Delta m_{\Lambda_b(5920)^0}$ [MeV]	300.479 ± 0.019	
$m_{\Lambda_b(5920)^0} - m_{\Lambda_b(5912)^0}$ [MeV]	7.896 ± 0.034	

Table 3. Results of the combined fit to the low-mass $\Lambda_b^0 \pi \pi$ spectra.

Source	$\Delta m_{\Lambda_b^{**0}}$ [MeV]	$\Gamma_{\Lambda_b^{**0}}$ [MeV]	$\Delta m_{\Lambda_b(1P)^0}$ [MeV]
Fit model			
Signal parameterisation	0.50	1.50	
Background parameterisation	0.03	0.25	
Fit range	0.10	0.30	
$\Lambda_b(1D)^0$ parameters			
Momentum scale uncertainty	0.08	—	0.010
Sum in quadrature	0.52	1.55	0.010

Table 4. Summary of systematic uncertainties for the mass difference with respect to the ground state Λ_b^0 and natural width of the Λ_b^{**0} state and the mass-differences for the $\Lambda_b(5912)^0$ and $\Lambda_b(5920)^0$ states, $\Delta m_{\Lambda_b(1P)^0}$.

three-body phase-space decays, while figure 4 suggests some contribution from decays via the intermediate $\Sigma_b^{(*)\pm}\pi^\mp$ states. To assess the associated systematic uncertainty, the fit is repeated using a more complicated function that in addition to nonresonant decays, accounts for the P-wave decays via an intermediate $\Sigma_b^{(*)\pm}\pi^\mp$ state, but ignores interference effects, constructed using the three-particle unitarity constraint approximated in the quasi-two-body interaction model [51]

$$\mathfrak{S}'\left(m|m_0, \Gamma_{\text{NR}}, \Gamma_{\Sigma_b\pi}, \Gamma_{\Sigma_b^*\pi}\right) \propto \frac{\Gamma(m)}{(m_0^2 - m^2)^2 + m_0^2 \Gamma^2(m)}, \quad (6.1)$$

where the mass-dependent width $\Gamma(m)$ is defined as

$$\Gamma(m) = \Gamma_{\text{NR}} \frac{\rho_3(m)}{\rho_3(m_0)} + \Gamma_{\Sigma_b\pi} \frac{\rho_{\Sigma_b\pi}(m)}{\rho_{\Sigma_b\pi}(m_0)} + \Gamma_{\Sigma_b^*\pi} \frac{\rho_{\Sigma_b^*\pi}(m)}{\rho_{\Sigma_b^*\pi}(m_0)}.$$

The quasi-two-body phase-space functions $\rho_{\Sigma_b^{(*)}\pi}(m)$ for the decays via the intermediate $\Sigma_b\pi$ and $\Sigma_b^*\pi$ states are

$$\rho_{\Sigma_b^{(*)}\pi}(m) = \int_{(m_\pi + m_{\Lambda_b^0})^2}^{(m - m_\pi)^2} \frac{\left(\frac{2p}{m} \frac{2q}{\sqrt{s}} \frac{R^2 p^2}{1 + R^2 p^2} \frac{R^2 q^2}{1 + R^2 q^2}\right)}{(m_{\Sigma_b^{(*)}}^2 - s)^2 + m_{\Sigma_b^{(*)}}^2 \Gamma_{\Sigma_b^{(*)}}^2(s)} ds,$$

$$\Gamma'_{\Sigma_b^{(*)}}(s) = \Gamma_{\Sigma_b^{(*)}} \frac{m_{\Sigma_b^{(*)}}}{\sqrt{s}} \left(\frac{q}{q_0}\right)^3 \left(\frac{1 + R^2 q^2}{1 + R^2 q_0^2}\right)^2,$$

where s stands for a squared mass of the $\Lambda_b^0\pi$ pair forming the $\Sigma_b^{(*)}$ resonance, p denotes the momenta of the pion in the P-wave decay $\Lambda_b^{**0} \rightarrow \Sigma_b^{(*)}\pi$, q denotes the momenta of the pion in the decay $\Sigma_b^{(*)} \rightarrow \Lambda_b^0\pi$, q_0 is the value of q at $s = m_{\Sigma_b^{(*)}}^2$, $R = 3.5 \text{ GeV}^{-1}$ corresponds to the breakup momentum of the P-wave Blatt-Weisskopf centrifugal barrier

factor [52], $m_{\Sigma_b^{(*)}}$ and $\Gamma_{\Sigma_b^{(*)}}$ are known mass and width of the $\Sigma_b^{(*)}$ states [7]. The function is reparameterised as

$$\begin{aligned}\Gamma_{\text{NR}} &= (1 - \alpha - \beta) \Gamma, \\ \Gamma_{\Sigma_b \pi} &= \alpha \Gamma, \\ \Gamma_{\Sigma_b^* \pi} &= \beta \Gamma,\end{aligned}$$

where the non-negative parameters α and β account for the relative contributions from the $\Lambda_b^{**0} \rightarrow \Sigma_b^\pm \pi^\mp$ and $\Lambda_b^{**0} \rightarrow \Sigma_b^{*\pm} \pi^\mp$ decays, respectively. A series of fits is performed with parameters α and β varied within the ranges $0 \leq \alpha < 0.2$, $0 \leq \beta < 0.2$, and $\alpha + \beta \leq 0.3$, consistent with figure 4. The mass of the Λ_b^{**0} state is found to be very stable with respect to such variations. The fitted mass does not change more than 0.5 MeV while the fitted width increases up to 1.5 MeV. These values are taken as systematic uncertainties due to the signal parameterisation. The nominal fit does not take the variations of the detector efficiency with the $\Lambda_b^0 \pi^+ \pi^-$ mass into account. An alternative fit is performed where the signal shape is multiplied by the efficiency function obtained from simulation. The difference with the nominal fit is added to the uncertainty on the signal parameterisation. Alternative parameterisations of the detector resolution functions, namely a symmetric variant of an Apollonios function [53], a double-sided Crystal Ball function [46], a modified Novosibirsk function [54, 55], a Student's t -distribution and a hyperbolic secant function, cause negligible variation for the measured mass and width of the Λ_b^{**0} state. The signal parameterisation uncertainty in the measurement of the masses of the low-mass states is negligible.

The uncertainty in the combinatorial background shape parameterisation is accounted for by varying the degree of the polynomial functions from 3 to 4. The uncertainty in the $\Sigma_b \pi$ and $\Sigma_b^* \pi$ background functions is evaluated by modifying the parameters of the exponential parameterisation within the limits allowed by the fits to the background-subtracted $\Sigma_b^{(*)} \pi$ spectra. In order to assess a possible sensitivity of the fit parameters to the features of the background shape not accounted for by the variations mentioned above, fits are performed in narrower and broader $\Lambda_b^0 \pi \pi$ regions and variations are included as an additional source of systematic uncertainty.

To assess the effect of the fixed parameters of the narrow $\Lambda_b(6146)^0$ and $\Lambda_b(6152)^0$ states from the previous analysis [10] in the higher-mass fit, the fits are performed with the masses and the widths of each of the two states left free to vary one by one. The resulting variations of the Λ_b^{**0} parameters are found to be negligible.

The effect of the calibration of the momentum scale is evaluated by varying the scale within its known uncertainty [8, 10, 26]. All systematic uncertainties for the mass difference $m_{\Lambda_b(5920)^0} - m_{\Lambda_b(5912)^0}$ are found to be negligible.

The upper limits on the natural widths of the $\Lambda_b(5912)^0$ and $\Lambda_b(5920)^0$ states are obtained by performing profile likelihood scans. In the calculation of the likelihood, the uncertainties in the knowledge of mass resolution are included by using various resolution models, as listed above, and by varying the mass-resolution scaling factor obtained from

simulations within 5% [10, 56, 57] and the maximum upper limits across all variations are reported.

7 Results and summary

Using the LHCb data set taken in 2011–2018, corresponding to an integrated luminosity of 9fb^{-1} collected in pp collisions at centre-of-mass energies of 7, 8 and 13 TeV, the $\Lambda_b^0\pi^+\pi^-$ mass spectrum is studied with Λ_b^0 baryons reconstructed in the $\Lambda_b^0 \rightarrow \Lambda_c^+\pi^-$ and $\Lambda_b^0 \rightarrow J/\psi pK^-$ decay modes. A new broad resonance-like state is observed with a statistical significance exceeding 14 and 7 standard deviations for $\Lambda_b^0\pi^+\pi^-$ samples reconstructed using the $\Lambda_b^0 \rightarrow \Lambda_c^+\pi^-$ and $\Lambda_b^0 \rightarrow J/\psi pK^-$ decay modes, respectively. The mass difference with respect to the Λ_b^0 mass and natural width of the state are determined from a combined fit to both samples and are found to be

$$\begin{aligned}\Delta m_{\Lambda_b^{**0}} &= 452.7 \pm 2.9 \pm 0.5 \text{ MeV}, \\ \Gamma_{\Lambda_b^{**0}} &= 72 \pm 11 \pm 2 \text{ MeV},\end{aligned}$$

where the first uncertainty is statistical and the second systematic. Taking the mass of the Λ_b^0 baryon $m_{\Lambda_b^0} = 5619.62 \pm 0.16 \pm 0.13 \text{ MeV}$ [48], obtained by a combination of measurements at the LHCb experiment in $\Lambda_b^0 \rightarrow \chi_{c1,2}pK^-$ [48], $\Lambda_b^0 \rightarrow \psi(2S)pK^-$, $\Lambda_b^0 \rightarrow J/\psi \pi^+\pi^- pK^-$ [58] and $\Lambda_b^0 \rightarrow J/\psi \Lambda$ decay modes [25, 59], and accounting for the correlated systematic uncertainty, the mass of the Λ_b^{**0} state is found to be

$$m_{\Lambda_b^{**0}} = 6072.3 \pm 2.9 \pm 0.6 \pm 0.2 \text{ MeV},$$

where the last uncertainty is due to that on the mass of the Λ_b^0 baryon. The new resonance is consistent with the broad excess of events reported by the CMS collaboration [15] and the measured mass and width agree with expectations for the $\Lambda_b(2S)^0$ state [16–18, 60, 61].

Several excited $\Sigma_b(1P)$ states are expected with a mass close to the measured value, but the partial decay widths for $\Sigma_b(1P)$ states into $\Lambda_b^0\pi\pi$ are predicted to be very small [62]. If the observed broad peak corresponds to the $\Sigma_b(1P)^{(*)0}$ state, two peaks with similar masses and widths and significantly larger yields should be visible in the $\Lambda_b^0\pi^\pm$ mass spectra due to decays of the charged isospin partners $\Sigma_b(1P)^{(*)\pm} \rightarrow \Lambda_b^0\pi^\pm$. However, no signs of states with such a mass and width, and large production yields are observed in the analysis of the $\Lambda_b^0\pi^\pm$ mass spectra; the observed $\Sigma_b(6097)^\pm$ states have significantly smaller natural width and relatively small yields [7]. It cannot be excluded that the observed broad structure corresponds to a superposition of more than one narrow states, but the interpretation of these states as excited Σ_b resonances is disfavoured.

The mass differences for the $\Lambda_b(5912)^0$ and $\Lambda_b(5920)^0$ states with respect to the mass of the Λ_b^0 baryon are measured to be

$$\begin{aligned}\Delta m_{\Lambda_b(5912)^0} &= 292.589 \pm 0.029 \pm 0.010 \text{ MeV}, \\ \Delta m_{\Lambda_b(5920)^0} &= 300.492 \pm 0.019 \pm 0.010 \text{ MeV},\end{aligned}$$

and the corresponding masses are

$$\begin{aligned} m_{\Lambda_b(5912)^0} &= 5912.21 \pm 0.03 \pm 0.01 \pm 0.21 \text{ MeV} , \\ m_{\Lambda_b(5920)^0} &= 5920.11 \pm 0.02 \pm 0.01 \pm 0.21 \text{ MeV} , \end{aligned}$$

where the last uncertainty is due to imprecise knowledge of the Λ_b^0 mass. The mass splitting between the narrow states is

$$m_{\Lambda_b(5920)^0} - m_{\Lambda_b(5912)^0} = 7.896 \pm 0.034 \text{ MeV} .$$

The following upper limits on the natural widths are obtained:

$$\begin{aligned} \Gamma_{\Lambda_b(5912)^0} &< 0.25 \text{ (0.28) MeV} , \\ \Gamma_{\Lambda_b(5920)^0} &< 0.19 \text{ (0.20) MeV} , \end{aligned}$$

at 90% (95%) confidence level, respectively. The measurements of the parameters of the $\Lambda_b(5912)^0$ and $\Lambda_b(5920)^0$ states are about four times more precise and supersede those reported in ref. [8].

Acknowledgments

We express our gratitude to our colleagues in the CERN accelerator departments for the excellent performance of the LHC. We thank the technical and administrative staff at the LHCb institutes. We acknowledge support from CERN and from the national agencies: CAPES, CNPq, FAPERJ and FINEP (Brazil); MOST and NSFC (China); CNRS/IN2P3 (France); BMBF, DFG and MPG (Germany); INFN (Italy); NWO (Netherlands); MNiSW and NCN (Poland); MEN/IFA (Romania); MSHE (Russia); MinECo (Spain); SNSF and SER (Switzerland); NASU (Ukraine); STFC (United Kingdom); DOE NP and NSF (USA). We acknowledge the computing resources that are provided by CERN, IN2P3 (France), KIT and DESY (Germany), INFN (Italy), SURF (Netherlands), PIC (Spain), GridPP (United Kingdom), RRCKI and Yandex LLC (Russia), CSCS (Switzerland), IFIN-HH (Romania), CBPF (Brazil), PL-GRID (Poland) and OSC (USA). We are indebted to the communities behind the multiple open-source software packages on which we depend. Individual groups or members have received support from AvH Foundation (Germany); EPLANET, Marie Skłodowska-Curie Actions and ERC (European Union); ANR, Labex P2IO and OCEVU, and Région Auvergne-Rhône-Alpes (France); Key Research Program of Frontier Sciences of CAS, CAS PIFI, and the Thousand Talents Program (China); RFBR, RSF and Yandex LLC (Russia); GVA, XuntaGal and GENCAT (Spain); the Royal Society and the Leverhulme Trust (United Kingdom).

Open Access. This article is distributed under the terms of the Creative Commons Attribution License ([CC-BY 4.0](https://creativecommons.org/licenses/by/4.0/)), which permits any use, distribution and reproduction in any medium, provided the original author(s) and source are credited.

References

- [1] M. Gell-Mann, *A Schematic Model of Baryons and Mesons*, *Phys. Lett.* **8** (1964) 214 [[INSPIRE](#)].
- [2] G. Zweig, *An SU_3 model for strong interaction symmetry and its breaking; Version 1*, *CERN-TH-401* (1964).
- [3] G. Zweig, *An SU_3 model for strong interaction symmetry and its breaking; Version 2*, *CERN-TH-412* (1964).
- [4] PARTICLE DATA GROUP collaboration, *Review of Particle Physics*, *Phys. Rev. D* **98** (2018) 030001 [[INSPIRE](#)].
- [5] CDF collaboration, *First observation of heavy baryons Σ_b and Σ_b^** , *Phys. Rev. Lett.* **99** (2007) 202001 [[arXiv:0706.3868](#)] [[INSPIRE](#)].
- [6] CDF collaboration, *Measurement of the masses and widths of the bottom baryons Σ_b^\pm and $\Sigma_b^{*\pm}$* , *Phys. Rev. D* **85** (2012) 092011 [[arXiv:1112.2808](#)] [[INSPIRE](#)].
- [7] LHCb collaboration, *Observation of two resonances in the $\Lambda_b^0 \pi^\pm$ systems and precise measurement of Σ_b^\pm and $\Sigma_b^{*\pm}$ properties*, *Phys. Rev. Lett.* **122** (2019) 012001 [[arXiv:1809.07752](#)] [[INSPIRE](#)].
- [8] LHCb collaboration, *Observation of excited Λ_b^0 baryons*, *Phys. Rev. Lett.* **109** (2012) 172003 [[arXiv:1205.3452](#)] [[INSPIRE](#)].
- [9] CDF collaboration, *Evidence for a bottom baryon resonance Λ_b^{*0} in CDF data*, *Phys. Rev. D* **88** (2013) 071101 [[arXiv:1308.1760](#)] [[INSPIRE](#)].
- [10] LHCb collaboration, *Observation of new resonances in the $\Lambda_b^0 \pi^+ \pi^-$ system*, *Phys. Rev. Lett.* **123** (2019) 152001 [[arXiv:1907.13598](#)] [[INSPIRE](#)].
- [11] B. Chen, S.-Q. Luo, X. Liu and T. Matsuki, *Ongoing construction to 1D bottom baryons by the observed $\Lambda_b(6146)^0$ and $\Lambda_b(6152)^0$ states*, *Phys. Rev. D* **100** (2019) 094032 [[arXiv:1910.03318](#)] [[INSPIRE](#)].
- [12] H.-M. Yang, H.-X. Chen, E.-L. Cui, A. Hosaka and Q. Mao, *Decay properties of P-wave heavy baryons accompanied by vector mesons within light-cone sum rules*, *Eur. Phys. J. C* **80** (2020) 80 [[arXiv:1909.13575](#)] [[INSPIRE](#)].
- [13] K.-L. Wang, Q.-F. Lü and X.-H. Zhong, *Interpretation of the newly observed $\Lambda_b(6146)^0$ and $\Lambda_b(6152)^0$ states in a chiral quark model*, *Phys. Rev. D* **100** (2019) 114035 [[arXiv:1908.04622](#)] [[INSPIRE](#)].
- [14] W. Liang, Q.-F. Lü and X.-H. Zhong, *Canonical interpretation of the newly observed $\Lambda_b(6146)^0$ and $\Lambda_b(6152)^0$ via strong decay behaviors*, *Phys. Rev. D* **100** (2019) 054013 [[arXiv:1908.00223](#)] [[INSPIRE](#)].
- [15] CMS collaboration, *Study of excited Λ_b^0 states decaying to $\Lambda_b^0 \pi^+ \pi^-$ in proton-proton collisions at $\sqrt{s} = 13$ TeV*, *Phys. Lett. B* **803** (2020) 135345 [[arXiv:2001.06533](#)] [[INSPIRE](#)].
- [16] S. Capstick and N. Isgur, *Baryons in a relativized quark model with chromodynamics*, *AIP Conf. Proc.* **132** (1985) 267 [[INSPIRE](#)].
- [17] W. Roberts and M. Pervin, *Heavy baryons in a quark model*, *Int. J. Mod. Phys. A* **23** (2008) 2817 [[arXiv:0711.2492](#)] [[INSPIRE](#)].

- [18] D. Ebert, R.N. Faustov and V.O. Galkin, *Spectroscopy and Regge trajectories of heavy baryons in the relativistic quark-diquark picture*, *Phys. Rev. D* **84** (2011) 014025 [[arXiv:1105.0583](#)] [[INSPIRE](#)].
- [19] B. Chen, K.-W. Wei and A. Zhang, *Investigation of Λ_Q and Ξ_Q baryons in the heavy quark-light diquark picture*, *Eur. Phys. J. A* **51** (2015) 82 [[arXiv:1406.6561](#)] [[INSPIRE](#)].
- [20] LHCb collaboration, *The LHCb detector at the LHC*, 2008 *JINST* **3** S08005 [[INSPIRE](#)].
- [21] LHCb collaboration, *LHCb detector performance*, *Int. J. Mod. Phys. A* **30** (2015) 1530022 [[arXiv:1412.6352](#)] [[INSPIRE](#)].
- [22] R. Aaij et al., *Performance of the LHCb Vertex Locator*, 2014 *JINST* **9** P09007 [[arXiv:1405.7808](#)] [[INSPIRE](#)].
- [23] R. Arink et al., *Performance of the LHCb Outer Tracker*, 2014 *JINST* **9** P01002 [[arXiv:1311.3893](#)] [[INSPIRE](#)].
- [24] P. d'Argent et al., *Improved performance of the LHCb Outer Tracker in LHC Run 2*, 2017 *JINST* **12** P11016 [[arXiv:1708.00819](#)] [[INSPIRE](#)].
- [25] LHCb collaboration, *Measurements of the Λ_b^0 , Ξ_b^- , and Ω_b^- baryon masses*, *Phys. Rev. Lett.* **110** (2013) 182001 [[arXiv:1302.1072](#)] [[INSPIRE](#)].
- [26] LHCb collaboration, *Precision measurement of D meson mass differences*, *JHEP* **06** (2013) 065 [[arXiv:1304.6865](#)] [[INSPIRE](#)].
- [27] M. Adinolfi et al., *Performance of the LHCb RICH detector at the LHC*, *Eur. Phys. J. C* **73** (2013) 2431 [[arXiv:1211.6759](#)] [[INSPIRE](#)].
- [28] A.A. Alves Jr. et al., *Performance of the LHCb muon system*, 2013 *JINST* **8** P02022 [[arXiv:1211.1346](#)] [[INSPIRE](#)].
- [29] R. Aaij et al., *The LHCb trigger and its performance in 2011*, 2013 *JINST* **8** P04022 [[arXiv:1211.3055](#)] [[INSPIRE](#)].
- [30] V.V. Gligorov and M. Williams, *Efficient, reliable and fast high-level triggering using a bonsai boosted decision tree*, 2013 *JINST* **8** P02013 [[arXiv:1210.6861](#)] [[INSPIRE](#)].
- [31] T. Likhomanenko, P. Ilten, E. Khairullin, A. Rogozhnikov, A. Ustyuzhanin and M. Williams, *LHCb topological trigger reoptimization*, *J. Phys. Conf. Ser.* **664** (2015) 082025 [[arXiv:1510.00572](#)] [[INSPIRE](#)].
- [32] T. Sjöstrand, S. Mrenna and P.Z. Skands, *PYTHIA 6.4 physics and manual*, *JHEP* **05** (2006) 026 [[hep-ph/0603175](#)] [[INSPIRE](#)].
- [33] LHCb collaboration, *Handling of the generation of primary events in GAUSS, the LHCb simulation framework*, *J. Phys. Conf. Ser.* **331** (2011) 032047 [[INSPIRE](#)].
- [34] D.J. Lange, *The EVTGEN particle decay simulation package*, *Nucl. Instrum. Meth. A* **462** (2001) 152 [[INSPIRE](#)].
- [35] P. Golonka and Z. Was, *PHOTOS Monte Carlo: A precision tool for QED corrections in Z and W decays*, *Eur. Phys. J. C* **45** (2006) 97 [[hep-ph/0506026](#)] [[INSPIRE](#)].
- [36] GEANT4 collaboration, *GEANT4 developments and applications*, *IEEE Trans. Nucl. Sci.* **53** (2006) 270 [[INSPIRE](#)].
- [37] GEANT4 collaboration, *GEANT4: A simulation toolkit*, *Nucl. Instrum. Meth. A* **506** (2003) 250 [[INSPIRE](#)].

- [38] LHCb collaboration, *The LHCb simulation application, GAUSS: Design, evolution and experience*, *J. Phys. Conf. Ser.* **331** (2011) 032023 [[INSPIRE](#)].
- [39] L. Breiman, J.H. Friedman, R.A. Olshen and C.J. Stone, *Classification and regression trees*, Wadsworth international group, Belmont, California, U.S.A., (1984).
- [40] Y. Freund and R.E. Schapire, *A decision-theoretic generalization of on-line learning and an application to boosting*, *J. Comput. Syst. Sci.* **55** (1997) 119.
- [41] H. Voss, A. Hocker, J. Stelzer and F. Tegenfeldt, TMVA — *Toolkit for multivariate data analysis*, *PoS ACAT* (2007) 040 [[INSPIRE](#)].
- [42] A. Hocker et al., TMVA 4 — *Toolkit for multivariate data analysis. Users Guide*, [physics/0703039](#) [[INSPIRE](#)].
- [43] W.D. Hulsbergen, *Decay chain fitting with a Kalman filter*, *Nucl. Instrum. Meth. A* **552** (2005) 566 [[physics/0503191](#)] [[INSPIRE](#)].
- [44] M. Pivk and F.R. Le Diberder, SPLOT: *A statistical tool to unfold data distributions*, *Nucl. Instrum. Meth. A* **555** (2005) 356 [[physics/0402083](#)] [[INSPIRE](#)].
- [45] S. Geisser, *Predictive inference: An introduction*, Monographs on statistics and applied probability, Chapman & Hall, New York, U.S.A., (1993).
- [46] T. Skwarnicki, *A study of the radiative cascade transitions between the Υ' and Υ resonances*, Ph.D. Thesis, Institute of Nuclear Physics, Krakow, Poland (1986).
- [47] G. Punzi, *Sensitivity of searches for new signals and its optimization*, [physics/0308063](#) [[INSPIRE](#)].
- [48] LHCb collaboration, *Observation of the decays $\Lambda_b^0 \rightarrow \chi_{c1} p K^-$ and $\Lambda_b^0 \rightarrow \chi_{c2} p K^-$* , *Phys. Rev. Lett.* **119** (2017) 062001 [[arXiv:1704.07900](#)] [[INSPIRE](#)].
- [49] G. Källén, *Elementary particle physics*, Addison-Wesley, Reading, Massachusetts, U.S.A. (1964).
- [50] S.S. Wilks, *The large-sample distribution of the likelihood ratio for testing composite hypotheses*, *Ann. Math. Stat.* **9** (1938) 60.
- [51] M. Mikhasenko et al., *Three-body scattering: ladders and resonances*, *JHEP* **08** (2019) 080 [[arXiv:1904.11894](#)] [[INSPIRE](#)].
- [52] J.M. Blatt and V.F. Weisskopf, *Theoretical nuclear physics*, Springer, New York, (1952), [DOI](#).
- [53] D. Martínez Santos and F. Dupertuis, *Mass distributions marginalized over per-event errors*, *Nucl. Instrum. Meth. A* **764** (2014) 150 [[arXiv:1312.5000](#)] [[INSPIRE](#)].
- [54] A. Bukin, *Fitting function for asymmetric peaks* [arXiv:0711.4449](#).
- [55] BABAR collaboration, *Branching fraction measurements of the color-suppressed decays $\bar{B}^0 \rightarrow D^{(*)0} \pi^0$, $D^{(*)0} \eta$, $D^{(*)0} \omega$, and $D^{(*)0} \eta'$ and measurement of the polarization in the decay $\bar{B}^0 \rightarrow D^{*0} \omega$* , *Phys. Rev. D* **84** (2011) 112007 [*Erratum* *ibid.* **87** (2013) 039901] [[arXiv:1107.5751](#)] [[INSPIRE](#)].
- [56] LHCb collaboration, *χ_{c1} and χ_{c2} resonance parameters with the decays $\chi_{c1,2} \rightarrow J/\psi \mu^+ \mu^-$* , *Phys. Rev. Lett.* **119** (2017) 221801 [[arXiv:1709.04247](#)] [[INSPIRE](#)].
- [57] LHCb collaboration, *Near-threshold $D\bar{D}$ spectroscopy and observation of a new charmonium state*, *JHEP* **07** (2019) 035 [[arXiv:1903.12240](#)] [[INSPIRE](#)].

- [58] LHCb collaboration, *Observation of $\Lambda_b^0 \rightarrow \psi(2S)pK^-$ and $\Lambda_b^0 \rightarrow J/\psi \pi^+ \pi^- pK^-$ decays and a measurement of the Λ_b^0 baryon mass*, *JHEP* **05** (2016) 132 [[arXiv:1603.06961](#)] [[INSPIRE](#)].
- [59] LHCb collaboration, *Measurement of b-hadron masses*, *Phys. Lett. B* **708** (2012) 241 [[arXiv:1112.4896](#)] [[INSPIRE](#)].
- [60] Y. Yamaguchi, S. Ohkoda, A. Hosaka, T. Hyodo and S. Yasui, *Heavy quark symmetry in multihadron systems*, *Phys. Rev. D* **91** (2015) 034034 [[arXiv:1402.5222](#)] [[INSPIRE](#)].
- [61] B. Chen and X. Liu, *Assigning the newly reported $\Sigma_b(6097)$ as a P-wave excited state and predicting its partners*, *Phys. Rev. D* **98** (2018) 074032 [[arXiv:1810.00389](#)] [[INSPIRE](#)].
- [62] C. Mu, X. Wang, X.-L. Chen, X. Liu and S.-L. Zhu, *Dipion decays of heavy baryons*, *Chin. Phys. C* **38** (2014) 113101 [[arXiv:1405.3128](#)] [[INSPIRE](#)].

The LHCb collaboration

R. Aaij³¹, C. Abellán Beteta⁴⁹, T. Ackernley⁵⁹, B. Adeva⁴⁵, M. Adinolfi⁵³, H. Afsharnia⁹, C.A. Aidala⁸⁰, S. Aiola²⁵, Z. Ajaltouni⁹, S. Akar⁶⁶, P. Albicocco²², J. Albrecht¹⁴, F. Alessio⁴⁷, M. Alexander⁵⁸, A. Alfonso Alberio⁴⁴, G. Alkhazov³⁷, P. Alvarez Cartelle⁶⁰, A.A. Alves Jr⁴⁵, S. Amato², Y. Amhis¹¹, L. An²¹, L. Anderlini²¹, G. Andreassi⁴⁸, M. Andreotti²⁰, F. Archilli¹⁶, A. Artamonov⁴³, M. Artuso⁶⁷, K. Arzymatov⁴¹, E. Aslanides¹⁰, M. Atzeni⁴⁹, B. Audurier¹¹, S. Bachmann¹⁶, J.J. Back⁵⁵, S. Baker⁶⁰, V. Balagura^{11,b}, W. Baldini^{20,47}, A. Baranov⁴¹, R.J. Barlow⁶¹, S. Barsuk¹¹, W. Barter⁶⁰, M. Bartolini^{23,47,h}, F. Baryshnikov⁷⁷, J.M. Basels¹³, G. Bassi²⁸, V. Batzskaya³⁵, B. Batsukh⁶⁷, A. Battig¹⁴, A. Bay⁴⁸, M. Becker¹⁴, F. Bedeschi²⁸, I. Bediaga¹, A. Beiter⁶⁷, L.J. Bel³¹, V. Belavin⁴¹, S. Belin²⁶, V. Bellec⁴⁸, K. Belous⁴³, I. Belyaev³⁸, G. Bencivenni²², E. Ben-Haim¹², S. Benson³¹, S. Beranek¹³, A. Berezhnoy³⁹, R. Bernet⁴⁹, D. Berninghoff¹⁶, H.C. Bernstein⁶⁷, C. Bertella⁴⁷, E. Bertholet¹², A. Bertolin²⁷, C. Betancourt⁴⁹, F. Betti^{19,e}, M.O. Bettler⁵⁴, Ia. Bezshyiko⁴⁹, S. Bhasin⁵³, J. Bhom³³, M.S. Bieker¹⁴, S. Bifani⁵², P. Billoir¹², A. Bizzeti^{21,u}, M. Bjørn⁶², M.P. Blago⁴⁷, T. Blake⁵⁵, F. Blanc⁴⁸, S. Blusk⁶⁷, D. Bobulska⁵⁸, V. Bocci³⁰, O. Boente Garcia⁴⁵, T. Boettcher⁶³, A. Boldyrev⁷⁸, A. Bondar^{42,x}, N. Bondar³⁷, S. Borghi^{61,47}, M. Borisyak⁴¹, M. Borsato¹⁶, J.T. Borsuk³³, T.J.V. Bowcock⁵⁹, C. Bozzi²⁰, M.J. Bradley⁶⁰, S. Braun¹⁶, A. Brea Rodriguez⁴⁵, M. Brodski⁴⁷, J. Brodzicka³³, A. Brossa Gonzalo⁵⁵, D. Brundu²⁶, E. Buchanan⁵³, A. Büchler-Germann⁴⁹, A. Buonauro⁴⁹, C. Burr⁴⁷, A. Bursche²⁶, A. Butkevich⁴⁰, J.S. Butter³¹, J. Buytaert⁴⁷, W. Byczynski⁴⁷, S. Cadeddu²⁶, H. Cai⁷², R. Calabrese^{20,g}, L. Calero Diaz²², S. Cali²², R. Calladine⁵², M. Calvi^{24,i}, M. Calvo Gomez^{44,m}, P. Camargo Magalhaes⁵³, A. Camboni^{44,m}, P. Campana²², D.H. Campora Perez³¹, A.F. Campoverde Quezada⁵, L. Capriotti^{19,e}, A. Carbone^{19,e}, G. Carboni²⁹, R. Cardinale^{23,h}, A. Cardini²⁶, I. Carli⁶, P. Carniti^{24,i}, K. Carvalho Akiba³¹, A. Casais Vidal⁴⁵, G. Casse⁵⁹, M. Cattaneo⁴⁷, G. Cavallero⁴⁷, S. Celani⁴⁸, R. Cenci^{28,p}, J. Cerasoli¹⁰, M.G. Chapman⁵³, M. Charles^{12,47}, Ph. Charpentier⁴⁷, G. Chatzikonstantinidis⁵², M. Chefdeville⁸, V. Chekalina⁴¹, C. Chen³, S. Chen²⁶, A. Chernov³³, S.-G. Chitic⁴⁷, V. Chobanova⁴⁵, S. Cholak⁴⁸, M. Chruszcz³³, A. Chubykin³⁷, P. Ciambrone²², M.F. Cicala⁵⁵, X. Cid Vidal⁴⁵, G. Ciezarek⁴⁷, F. Cindolo¹⁹, P.E.L. Clarke⁵⁷, M. Clemencic⁴⁷, H.V. Cliff⁵⁴, J. Closier⁴⁷, J.L. Cobbledick⁶¹, V. Coco⁴⁷, J.A.B. Coelho¹¹, J. Cogan¹⁰, E. Cogneras⁹, L. Cojocariu³⁶, P. Collins⁴⁷, T. Colombo⁴⁷, A. Comerma-Montells¹⁶, A. Contu²⁶, N. Cooke⁵², G. Coombs⁵⁸, S. Coquereau⁴⁴, G. Corti⁴⁷, C.M. Costa Sobral⁵⁵, B. Couturier⁴⁷, D.C. Craik⁶³, J. Crkovská⁶⁶, A. Crocombe⁵⁵, M. Cruz Torres^{1,ab}, R. Currie⁵⁷, C.L. Da Silva⁶⁶, E. Dall'Occo¹⁴, J. Dalseno^{45,53}, C. D'Ambrosio⁴⁷, A. Danilina³⁸, P. d'Argent⁴⁷, A. Davis⁶¹, O. De Aguiar Francisco⁴⁷, K. De Bruyn⁴⁷, S. De Capua⁶¹, M. De Cian⁴⁸, J.M. De Miranda¹, L. De Paula², M. De Serio^{18,d}, P. De Simone²², J.A. de Vries³¹, C.T. Dean⁶⁶, W. Dean⁸⁰, D. Decamp⁸, L. Del Buono¹², B. Delaney⁵⁴, H.-P. Dembinski¹⁵, A. Dendek³⁴, V. Denysenko⁴⁹, D. Derkach⁷⁸, O. Deschamps⁹, F. Desse¹¹, F. Dettori^{26,f}, B. Dey⁷, A. Di Canto⁴⁷, P. Di Nezza²², S. Didenko⁷⁷, H. Dijkstra⁴⁷, V. Dobishuk⁵¹, F. Dordei²⁶, M. Dorigo^{28,y}, A.C. dos Reis¹, L. Douglas⁵⁸, A. Dovbnya⁵⁰, K. Dreimanis⁵⁹, M.W. Dudek³³, L. Dufour⁴⁷, G. Dujany¹², P. Durante⁴⁷, J.M. Durham⁶⁶, D. Dutta⁶¹, M. Dziewiecki¹⁶, A. Dziurda³³, A. Dzyuba³⁷, S. Easo⁵⁶, U. Egede⁶⁹, V. Egorychev³⁸, S. Eidelman^{42,x}, S. Eisenhardt⁵⁷, R. Ekelhof¹⁴, S. Ek-In⁴⁸, L. Eklund⁵⁸, S. Ely⁶⁷, A. Ene³⁶, E. Eppele⁶⁶, S. Escher¹³, S. Esen³¹, T. Evans⁴⁷, A. Falabella¹⁹, J. Fan³, N. Farley⁵², S. Farry⁵⁹, D. Fazzini¹¹, P. Fedin³⁸, M. Féo⁴⁷, P. Fernandez Declara⁴⁷, A. Fernandez Prieto⁴⁵, F. Ferrari^{19,e}, L. Ferreira Lopes⁴⁸, F. Ferreira Rodrigues², S. Ferreres Sole³¹, M. Ferrillo⁴⁹, M. Ferro-Luzzi⁴⁷, S. Filippov⁴⁰, R.A. Fini¹⁸, M. Fiorini^{20,g}, M. Firlej³⁴, K.M. Fischer⁶², C. Fitzpatrick⁴⁷, T. Fiutowski³⁴, F. Fleuret^{11,b}, M. Fontana⁴⁷, F. Fontanelli^{23,h}, R. Forty⁴⁷, V. Franco Lima⁵⁹, M. Franco Sevilla⁶⁵, M. Frank⁴⁷, C. Frei⁴⁷,

D.A. Friday⁵⁸, J. Fu^{25,q}, Q. Fuehring¹⁴, W. Funk⁴⁷, E. Gabriel⁵⁷, A. Gallas Torreira⁴⁵,
 D. Galli^{19,e}, S. Gallorini²⁷, S. Gambetta⁵⁷, Y. Gan³, M. Gandelman², P. Gandini²⁵, Y. Gao⁴,
 L.M. Garcia Martin⁴⁶, J. García Pardiñas⁴⁹, B. Garcia Plana⁴⁵, F.A. Garcia Rosales¹¹,
 L. Garrido⁴⁴, D. Gascon⁴⁴, C. Gaspar⁴⁷, D. Gerick¹⁶, E. Gersabeck⁶¹, M. Gersabeck⁶¹,
 T. Gershon⁵⁵, D. Gerstel¹⁰, Ph. Ghez⁸, V. Gibson⁵⁴, A. Gioventù⁴⁵, O.G. Girard⁴⁸,
 P. Gironella Gironell⁴⁴, L. Giubega³⁶, C. Giugliano²⁰, K. Gizdov⁵⁷, V.V. Gligorov¹², C. Göbel⁷⁰,
 E. Golobardes^{44,m}, D. Golubkov³⁸, A. Golutvin^{60,77}, A. Gomes^{1,a}, P. Gorbounov^{38,6},
 I.V. Gorelov³⁹, C. Gotti^{24,i}, E. Govorkova³¹, J.P. Grabowski¹⁶, R. Graciani Diaz⁴⁴,
 T. Grammatico¹², L.A. Granado Cardoso⁴⁷, E. Graugés⁴⁴, E. Graverini⁴⁸, G. Graziani²¹,
 A. Grecu³⁶, R. Greim³¹, P. Griffith²⁰, L. Grillo⁶¹, L. Gruber⁴⁷, B.R. Gruberg Cazon⁶², C. Gu³,
 E. Gushchin⁴⁰, A. Guth¹³, Yu. Guz^{43,47}, T. Gys⁴⁷, P. A. Günther¹⁶, T. Hadavizadeh⁶²,
 G. Haefeli⁴⁸, C. Haen⁴⁷, S.C. Haines⁵⁴, P.M. Hamilton⁶⁵, Q. Han⁷, X. Han¹⁶, T.H. Hancock⁶²,
 S. Hansmann-Menzemer¹⁶, N. Harnew⁶², T. Harrison⁵⁹, R. Hart³¹, C. Hasse¹⁴, M. Hatch⁴⁷,
 J. He⁵, M. Hecker⁶⁰, K. Heijhoff³¹, K. Heinicke¹⁴, A.M. Hennequin⁴⁷, K. Hennessy⁵⁹, L. Henry⁴⁶,
 J. Heuel¹³, A. Hicheur⁶⁸, D. Hill⁶², M. Hilton⁶¹, P.H. Hopchev⁴⁸, J. Hu¹⁶, W. Hu⁷, W. Huang⁵,
 W. Hulsbergen³¹, T. Humair⁶⁰, R.J. Hunter⁵⁵, M. Hushchyn⁷⁸, D. Hutchcroft⁵⁹, D. Hynds³¹,
 P. Ibis¹⁴, M. Idzik³⁴, P. Ilten⁵², A. Inglessi³⁷, K. Ivshin³⁷, R. Jacobsson⁴⁷, S. Jakobsen⁴⁷,
 E. Jans³¹, B.K. Jashal⁴⁶, A. Jawahery⁶⁵, V. Jevtic¹⁴, F. Jiang³, M. John⁶², D. Johnson⁴⁷,
 C.R. Jones⁵⁴, B. Jost⁴⁷, N. Jurik⁶², S. Kandybei⁵⁰, M. Karacson⁴⁷, J.M. Kariuki⁵³, N. Kazeev⁷⁸,
 M. Kecke¹⁶, F. Keizer^{54,47}, M. Kelsey⁶⁷, M. Kenzie⁵⁵, T. Ketel³², B. Khanji⁴⁷, A. Kharisova⁷⁹,
 K.E. Kim⁶⁷, T. Kirn¹³, V.S. Kirsebom⁴⁸, S. Klaver²², K. Klimaszewski³⁵, S. Kolliiev⁵¹,
 A. Kondybayeva⁷⁷, A. Konoplyannikov³⁸, P. Kopciwicz³⁴, R. Kopecna¹⁶, P. Koppenburg³¹,
 M. Korolev³⁹, I. Kostiuk^{31,51}, O. Kot⁵¹, S. Kotriakhova³⁷, L. Kravchuk⁴⁰, R.D. Krawczyk⁴⁷,
 M. Kreps⁵⁵, F. Kress⁶⁰, S. Kretzschmar¹³, P. Krokovny^{42,x}, W. Krupa³⁴, W. Krzemien³⁵,
 W. Kucewicz^{33,l}, M. Kucharczyk³³, V. Kudryavtsev^{42,x}, H.S. Kuindersma³¹, G.J. Kunde⁶⁶,
 T. Kvaratskheliya³⁸, D. Lacarrere⁴⁷, G. Lafferty⁶¹, A. Lai²⁶, D. Lancieri⁴⁹, J.J. Lane⁶¹,
 G. Lanfranchi²², C. Langenbruch¹³, O. Lantwin⁴⁹, T. Latham⁵⁵, F. Lazzari^{28,v}, C. Lazzeroni⁵²,
 R. Le Gac¹⁰, R. Lefèvre⁹, A. Leflat³⁹, O. Leroy¹⁰, T. Lesiak³³, B. Leverington¹⁶, H. Li⁷¹, L. Li⁶²,
 X. Li⁶⁶, Y. Li⁶, Z. Li⁶⁷, X. Liang⁶⁷, R. Lindner⁴⁷, V. Lisovskyi¹⁴, G. Liu⁷¹, X. Liu³, D. Loh⁵⁵,
 A. Loi²⁶, J. Lomba Castro⁴⁵, I. Longstaff⁵⁸, J.H. Lopes², G. Loustau⁴⁹, G.H. Lovell⁵⁴, Y. Lu⁶,
 D. Lucchesi^{27,o}, M. Lucio Martinez³¹, Y. Luo³, A. Lupato²⁷, E. Luppi^{20,g}, O. Lupton⁵⁵,
 A. Lusiani^{28,t}, X. Lyu⁵, S. Maccolini^{19,e}, F. Machefert¹¹, F. Maciuc³⁶, V. Macko⁴⁸,
 P. Mackowiak¹⁴, S. Maddrell-Mander⁵³, L.R. Madhan Mohan⁵³, O. Maev^{37,47}, A. Maevskiy⁷⁸,
 D. Maisuzenko³⁷, M.W. Majewski³⁴, S. Malde⁶², B. Malecki⁴⁷, A. Malinin⁷⁶, T. Maltsev^{42,x},
 H. Malygina¹⁶, G. Manca^{26,f}, G. Mancinelli¹⁰, R. Manera Escalero⁴⁴, D. Manuzzi^{19,e},
 D. Marangotto^{25,q}, J. Maratas^{9,w}, J.F. Marchand⁸, U. Marconi¹⁹, S. Mariani²¹,
 C. Marin Benito¹¹, M. Marinangeli⁴⁸, P. Marino⁴⁸, J. Marks¹⁶, P.J. Marshall⁵⁹, G. Martellotti³⁰,
 L. Martinazzoli⁴⁷, M. Martinelli^{24,i}, D. Martinez Santos⁴⁵, F. Martinez Vidal⁴⁶, A. Massafferri¹,
 M. Materok¹³, R. Matev⁴⁷, A. Mathad⁴⁹, Z. Mathe⁴⁷, V. Matiunin³⁸, C. Matteuzzi²⁴,
 K.R. Mattioli⁸⁰, A. Mauri⁴⁹, E. Maurice^{11,b}, M. McCann⁶⁰, L. McConnell¹⁷, A. McNab⁶¹,
 R. McNulty¹⁷, J.V. Mead⁵⁹, B. Meadows⁶⁴, C. Meaux¹⁰, G. Meier¹⁴, N. Meinert⁷⁴,
 D. Melnychuk³⁵, S. Meloni^{24,i}, M. Merk³¹, A. Merli²⁵, M. Mikhasenko⁴⁷, D.A. Milanes⁷³,
 E. Millard⁵⁵, M.-N. Minard⁸, O. Mineev³⁸, L. Minzoni^{20,g}, S.E. Mitchell⁵⁷, B. Mitreska⁶¹,
 D.S. Mitzel⁴⁷, A. Mödden¹⁴, A. Mogini¹², R.D. Moise⁶⁰, T. Mombächer¹⁴, I.A. Monroy⁷³,
 S. Monteil⁹, M. Morandin²⁷, G. Morello²², M.J. Morello^{28,t}, J. Moron³⁴, A.B. Morris¹⁰,
 A.G. Morris⁵⁵, R. Mountain⁶⁷, H. Mu³, F. Muheim⁵⁷, M. Mukherjee⁷, M. Mulder⁴⁷, D. Müller⁴⁷,
 K. Müller⁴⁹, C.H. Murphy⁶², D. Murray⁶¹, P. Muzzetto²⁶, P. Naik⁵³, T. Nakada⁴⁸,
 R. Nandakumar⁵⁶, T. Nanut⁴⁸, I. Nasteva², M. Needham⁵⁷, N. Neri^{25,q}, S. Neubert¹⁶,

N. Neufeld⁴⁷, R. Newcombe⁶⁰, T.D. Nguyen⁴⁸, C. Nguyen-Mau^{48,n}, E.M. Niel¹¹, S. Nieswand¹³, N. Nikitin³⁹, N.S. Nolte⁴⁷, C. Nunez⁸⁰, A. Oblakowska-Mucha³⁴, V. Obraztsov⁴³, S. Ogilvy⁵⁸, D.P. O’Hanlon⁵³, R. Oldeman^{26,f}, C.J.G. Onderwater⁷⁵, J. D. Osborn⁸⁰, A. Ossowska³³, J.M. Otalora Goicochea², T. Ovsiannikova³⁸, P. Owen⁴⁹, A. Oyanguren⁴⁶, P.R. Pais⁴⁸, T. Pajero^{28,t}, A. Palano¹⁸, M. Palutan²², G. Panshin⁷⁹, A. Papanestis⁵⁶, M. Pappagallo⁵⁷, L.L. Pappalardo^{20,g}, C. Pappenheimer⁶⁴, W. Parker⁶⁵, C. Parkes⁶¹, G. Passaleva^{21,47}, A. Pastore¹⁸, M. Patel⁶⁰, C. Patrignani^{19,e}, A. Pearce⁴⁷, A. Pellegrino³¹, M. Pepe Altarelli⁴⁷, S. Perazzini¹⁹, D. Pereima³⁸, P. Perret⁹, L. Pescatore⁴⁸, K. Petridis⁵³, A. Petrolini^{23,h}, A. Petrov⁷⁶, S. Petrucci⁵⁷, M. Petruzzio^{25,q}, B. Pietrzyk⁸, G. Pietrzyk⁴⁸, M. Pili⁶², D. Pinci³⁰, J. Pinzino⁴⁷, F. Pisani¹⁹, A. Piucci¹⁶, V. Placinta³⁶, S. Playfer⁵⁷, J. Plews⁵², M. Plo Casasus⁴⁵, F. Polci¹², M. Poli Lener²², M. Poliakova⁶⁷, A. Poluektov¹⁰, N. Polukhina^{77,c}, I. Polyakov⁶⁷, E. Polycarpo², G.J. Pomery⁵³, S. Ponce⁴⁷, A. Popov⁴³, D. Popov⁵², S. Poslavskii⁴³, K. Prasanth³³, L. Promberger⁴⁷, C. Prouve⁴⁵, V. Pugatch⁵¹, A. Puig Navarro⁴⁹, H. Pullen⁶², G. Punzi^{28,p}, W. Qian⁵, J. Qin⁵, R. Quagliani¹², B. Quintana⁸, N.V. Raab¹⁷, R.I. Rabadan Trejo¹⁰, B. Rachwal³⁴, J.H. Rademacker⁵³, M. Rama²⁸, M. Ramos Pernas⁴⁵, M.S. Rangel², F. Ratnikov^{41,78}, G. Raven³², M. Reboud⁸, F. Redi⁴⁸, F. Reiss¹², C. Remon Alepuz⁴⁶, Z. Ren³, V. Renaudin⁶², S. Ricciardi⁵⁶, D.S. Richards⁵⁶, S. Richards⁵³, K. Rinnert⁵⁹, P. Robbe¹¹, A. Robert¹², A.B. Rodrigues⁴⁸, E. Rodrigues⁶⁴, J.A. Rodriguez Lopez⁷³, M. Roehrken⁴⁷, S. Roiser⁴⁷, A. Rollings⁶², V. Romanovskiy⁴³, M. Romero Lamas⁴⁵, A. Romero Vidal⁴⁵, J.D. Roth⁸⁰, M. Rotondo²², M.S. Rudolph⁶⁷, T. Ruf⁴⁷, J. Ruiz Vidal⁴⁶, A. Ryzhikov⁷⁸, J. Ryzka³⁴, J.J. Saborido Silva⁴⁵, N. Sagidova³⁷, N. Sahoo⁵⁵, B. Saitta^{26,f}, C. Sanchez Gras³¹, C. Sanchez Mayordomo⁴⁶, R. Santacesaria³⁰, C. Santamarina Rios⁴⁵, M. Santimaria²², E. Santovetti^{29,j}, G. Sarpis⁶¹, A. Sarti³⁰, C. Satriano^{30,s}, A. Satta²⁹, M. Saur⁵, D. Savrina^{38,39}, L.G. Scantlebury Smead⁶², S. Schael¹³, M. Schellenberg¹⁴, M. Schiller⁵⁸, H. Schindler⁴⁷, M. Schmelling¹⁵, T. Schmelzer¹⁴, B. Schmidt⁴⁷, O. Schneider⁴⁸, A. Schopper⁴⁷, H.F. Schreiner⁶⁴, M. Schubiger³¹, S. Schulte⁴⁸, M.H. Schune¹¹, R. Schwemmer⁴⁷, B. Sciascia²², A. Sciubba^{30,k}, S. Sellam⁶⁸, A. Semennikov³⁸, A. Sergi^{52,47}, N. Serra⁴⁹, J. Serrano¹⁰, L. Sestini²⁷, A. Seuthe¹⁴, P. Seyfert⁴⁷, D.M. Shangase⁸⁰, M. Shapkin⁴³, L. Shchutka⁴⁸, T. Shears⁵⁹, L. Shekhtman^{42,x}, V. Shevchenko^{76,77}, E. Shmanin⁷⁷, J.D. Shupperd⁶⁷, B.G. Siddi²⁰, R. Silva Coutinho⁴⁹, L. Silva de Oliveira², G. Simi^{27,o}, S. Simone^{18,d}, I. Skiba²⁰, N. Skidmore¹⁶, T. Skwarnicki⁶⁷, M.W. Slater⁵², J.G. Smeaton⁵⁴, A. Smetkina³⁸, E. Smith¹³, I.T. Smith⁵⁷, M. Smith⁶⁰, A. Snoch³¹, M. Soares¹⁹, L. Soares Lavra⁹, M.D. Sokoloff⁶⁴, F.J.P. Soler⁵⁸, B. Souza De Paula², B. Spaan¹⁴, E. Spadaro Norella^{25,q}, P. Spradlin⁵⁸, F. Stagni⁴⁷, M. Stahl⁶⁴, S. Stahl⁴⁷, P. Stefko⁴⁸, O. Steinkamp⁴⁹, S. Stemmler¹⁶, O. Stenyakin⁴³, M. Stepanova³⁷, H. Stevens¹⁴, S. Stone⁶⁷, S. Stracka²⁸, M.E. Stramaglia⁴⁸, M. Straticiu³⁶, S. Strokov⁷⁹, J. Sun²⁶, L. Sun⁷², Y. Sun⁶⁵, P. Sviha⁶¹, K. Swientek³⁴, A. Szabelski³⁵, T. Szumlak³⁴, M. Szymanski⁴⁷, S. Taneja⁶¹, Z. Tang³, T. Tekampe¹⁴, F. Teubert⁴⁷, E. Thomas⁴⁷, K.A. Thomson⁵⁹, M.J. Tilley⁶⁰, V. Tisserand⁹, S. T’Jampens⁸, M. Tobin⁶, S. Tolk⁴⁷, L. Tomassetti^{20,g}, D. Tonelli²⁸, D. Torres Machado¹, D.Y. Tou¹², E. Tournefier⁸, M. Traill⁵⁸, M.T. Tran⁴⁸, E. Trifonova⁷⁷, C. Trippel⁴⁸, A. Trisovic⁵⁴, A. Tsaregorodtsev¹⁰, G. Tuci^{28,47,p}, A. Tully⁴⁸, N. Tuning³¹, A. Ukleja³⁵, A. Usachov³¹, A. Ustyuzhanin^{41,78}, U. Uwer¹⁶, A. Vagner⁷⁹, V. Vagnoni¹⁹, A. Valassi⁴⁷, G. Valenti¹⁹, M. van Beuzekom³¹, H. Van Hecke⁶⁶, E. van Herwijnen⁴⁷, C.B. Van Hulse¹⁷, M. van Veghel⁷⁵, R. Vazquez Gomez^{44,22}, P. Vazquez Regueiro⁴⁵, C. Vázquez Sierra³¹, S. Vecchi²⁰, J.J. Velthuis⁵³, M. Veltri^{21,r}, A. Venkateswaran⁶⁷, M. Vernet⁹, M. Veronesi³¹, M. Vesterinen⁵⁵, J.V. Viana Barbosa⁴⁷, D. Vieira⁶⁴, M. Vieites Diaz⁴⁸, H. Viemann⁷⁴, X. Vilasis-Cardona^{44,m}, A. Vitkovskiy³¹, A. Vollhardt⁴⁹, D. Vom Bruch¹², A. Vorobyev³⁷, V. Vorobyev^{42,x}, N. Voropaev³⁷, R. Waldi⁷⁴, J. Walsh²⁸, J. Wang³, J. Wang⁷², J. Wang⁶, M. Wang³, Y. Wang⁷, Z. Wang⁴⁹, D.R. Ward⁵⁴, H.M. Wark⁵⁹, N.K. Watson⁵²,

D. Websdale⁶⁰, A. Weiden⁴⁹, C. Weisser⁶³, B.D.C. Westhenry⁵³, D.J. White⁶¹, M. Whitehead¹³, D. Wiedner¹⁴, G. Wilkinson⁶², M. Wilkinson⁶⁷, I. Williams⁵⁴, M. Williams⁶³, M.R.J. Williams⁶¹, T. Williams⁵², F.F. Wilson⁵⁶, W. Wislicki³⁵, M. Witek³³, L. Witola¹⁶, G. Wormser¹¹, S.A. Wotton⁵⁴, H. Wu⁶⁷, K. Wyllie⁴⁷, Z. Xiang⁵, D. Xiao⁷, Y. Xie⁷, H. Xing⁷¹, A. Xu⁴, J. Xu⁵, L. Xu³, M. Xu⁷, Q. Xu⁵, Z. Xu⁴, Z. Yang³, Z. Yang⁶⁵, Y. Yao⁶⁷, L.E. Yeomans⁵⁹, H. Yin⁷, J. Yu^{7,aa}, X. Yuan⁶⁷, O. Yushchenko⁴³, K.A. Zarebski⁵², M. Zavertyaev^{15,c}, M. Zdybal³³, M. Zeng³, D. Zhang⁷, L. Zhang³, S. Zhang⁴, W.C. Zhang^{3,z}, Y. Zhang⁴⁷, A. Zhelezov¹⁶, Y. Zheng⁵, X. Zhou⁵, Y. Zhou⁵, X. Zhu³, V. Zhukov^{13,39}, J.B. Zonneveld⁵⁷, S. Zucchelli^{19,e}

¹ Centro Brasileiro de Pesquisas Físicas (CBPF), Rio de Janeiro, Brazil

² Universidade Federal do Rio de Janeiro (UFRJ), Rio de Janeiro, Brazil

³ Center for High Energy Physics, Tsinghua University, Beijing, China

⁴ School of Physics State Key Laboratory of Nuclear Physics and Technology, Peking University, Beijing, China

⁵ University of Chinese Academy of Sciences, Beijing, China

⁶ Institute Of High Energy Physics (IHEP), Beijing, China

⁷ Institute of Particle Physics, Central China Normal University, Wuhan, Hubei, China

⁸ Univ. Grenoble Alpes, Univ. Savoie Mont Blanc, CNRS, IN2P3-LAPP, Annecy, France

⁹ Université Clermont Auvergne, CNRS/IN2P3, LPC, Clermont-Ferrand, France

¹⁰ Aix Marseille Univ, CNRS/IN2P3, CPPM, Marseille, France

¹¹ Université Paris-Saclay, CNRS/IN2P3, IJCLab, Orsay, France

¹² LPNHE, Sorbonne Université, Paris Diderot Sorbonne Paris Cité, CNRS/IN2P3, Paris, France

¹³ I. Physikalisches Institut, RWTH Aachen University, Aachen, Germany

¹⁴ Fakultät Physik, Technische Universität Dortmund, Dortmund, Germany

¹⁵ Max-Planck-Institut für Kernphysik (MPIK), Heidelberg, Germany

¹⁶ Physikalisches Institut, Ruprecht-Karls-Universität Heidelberg, Heidelberg, Germany

¹⁷ School of Physics, University College Dublin, Dublin, Ireland

¹⁸ INFN Sezione di Bari, Bari, Italy

¹⁹ INFN Sezione di Bologna, Bologna, Italy

²⁰ INFN Sezione di Ferrara, Ferrara, Italy

²¹ INFN Sezione di Firenze, Firenze, Italy

²² INFN Laboratori Nazionali di Frascati, Frascati, Italy

²³ INFN Sezione di Genova, Genova, Italy

²⁴ INFN Sezione di Milano-Bicocca, Milano, Italy

²⁵ INFN Sezione di Milano, Milano, Italy

²⁶ INFN Sezione di Cagliari, Monserrato, Italy

²⁷ INFN Sezione di Padova, Padova, Italy

²⁸ INFN Sezione di Pisa, Pisa, Italy

²⁹ INFN Sezione di Roma Tor Vergata, Roma, Italy

³⁰ INFN Sezione di Roma La Sapienza, Roma, Italy

³¹ Nikhef National Institute for Subatomic Physics, Amsterdam, Netherlands

³² Nikhef National Institute for Subatomic Physics and VU University Amsterdam, Amsterdam, Netherlands

³³ Henryk Niewodniczanski Institute of Nuclear Physics Polish Academy of Sciences, Kraków, Poland

³⁴ AGH — University of Science and Technology, Faculty of Physics and Applied Computer Science, Kraków, Poland

³⁵ National Center for Nuclear Research (NCBJ), Warsaw, Poland

³⁶ Horia Hulubei National Institute of Physics and Nuclear Engineering, Bucharest-Magurele, Romania

³⁷ Petersburg Nuclear Physics Institute NRC Kurchatov Institute (PNPI NRC KI), Gatchina, Russia

³⁸ Institute of Theoretical and Experimental Physics NRC Kurchatov Institute (ITEP NRC KI), Moscow, Russia, Moscow, Russia

- ³⁹ *Institute of Nuclear Physics, Moscow State University (SINP MSU), Moscow, Russia*
- ⁴⁰ *Institute for Nuclear Research of the Russian Academy of Sciences (INR RAS), Moscow, Russia*
- ⁴¹ *Yandex School of Data Analysis, Moscow, Russia*
- ⁴² *Budker Institute of Nuclear Physics (SB RAS), Novosibirsk, Russia*
- ⁴³ *Institute for High Energy Physics NRC Kurchatov Institute (IHEP NRC KI), Protvino, Russia, Protvino, Russia*
- ⁴⁴ *ICCUB, Universitat de Barcelona, Barcelona, Spain*
- ⁴⁵ *Instituto Galego de Física de Altas Enerxías (IGFAE), Universidade de Santiago de Compostela, Santiago de Compostela, Spain*
- ⁴⁶ *Instituto de Física Corpuscular, Centro Mixto Universidad de Valencia — CSIC, Valencia, Spain*
- ⁴⁷ *European Organization for Nuclear Research (CERN), Geneva, Switzerland*
- ⁴⁸ *Institute of Physics, Ecole Polytechnique Fédérale de Lausanne (EPFL), Lausanne, Switzerland*
- ⁴⁹ *Physik-Institut, Universität Zürich, Zürich, Switzerland*
- ⁵⁰ *NSC Kharkiv Institute of Physics and Technology (NSC KIPT), Kharkiv, Ukraine*
- ⁵¹ *Institute for Nuclear Research of the National Academy of Sciences (KINR), Kyiv, Ukraine*
- ⁵² *University of Birmingham, Birmingham, United Kingdom*
- ⁵³ *H.H. Wills Physics Laboratory, University of Bristol, Bristol, United Kingdom*
- ⁵⁴ *Cavendish Laboratory, University of Cambridge, Cambridge, United Kingdom*
- ⁵⁵ *Department of Physics, University of Warwick, Coventry, United Kingdom*
- ⁵⁶ *STFC Rutherford Appleton Laboratory, Didcot, United Kingdom*
- ⁵⁷ *School of Physics and Astronomy, University of Edinburgh, Edinburgh, United Kingdom*
- ⁵⁸ *School of Physics and Astronomy, University of Glasgow, Glasgow, United Kingdom*
- ⁵⁹ *Oliver Lodge Laboratory, University of Liverpool, Liverpool, United Kingdom*
- ⁶⁰ *Imperial College London, London, United Kingdom*
- ⁶¹ *Department of Physics and Astronomy, University of Manchester, Manchester, United Kingdom*
- ⁶² *Department of Physics, University of Oxford, Oxford, United Kingdom*
- ⁶³ *Massachusetts Institute of Technology, Cambridge, MA, United States*
- ⁶⁴ *University of Cincinnati, Cincinnati, OH, United States*
- ⁶⁵ *University of Maryland, College Park, MD, United States*
- ⁶⁶ *Los Alamos National Laboratory (LANL), Los Alamos, United States*
- ⁶⁷ *Syracuse University, Syracuse, NY, United States*
- ⁶⁸ *Laboratory of Mathematical and Subatomic Physics, Constantine, Algeria, associated to ²*
- ⁶⁹ *School of Physics and Astronomy, Monash University, Melbourne, Australia, associated to ⁵⁵*
- ⁷⁰ *Pontifícia Universidade Católica do Rio de Janeiro (PUC-Rio), Rio de Janeiro, Brazil, associated to ²*
- ⁷¹ *Guangdong Provincial Key Laboratory of Nuclear Science, Institute of Quantum Matter, South China Normal University, Guangzhou, China, associated to ³*
- ⁷² *School of Physics and Technology, Wuhan University, Wuhan, China, associated to ³*
- ⁷³ *Departamento de Física, Universidad Nacional de Colombia, Bogota, Colombia, associated to ¹²*
- ⁷⁴ *Institut für Physik, Universität Rostock, Rostock, Germany, associated to ¹⁶*
- ⁷⁵ *Van Swinderen Institute, University of Groningen, Groningen, Netherlands, associated to ³¹*
- ⁷⁶ *National Research Centre Kurchatov Institute, Moscow, Russia, associated to ³⁸*
- ⁷⁷ *National University of Science and Technology “MISIS”, Moscow, Russia, associated to ³⁸*
- ⁷⁸ *National Research University Higher School of Economics, Moscow, Russia, associated to ⁴¹*
- ⁷⁹ *National Research Tomsk Polytechnic University, Tomsk, Russia, associated to ³⁸*
- ⁸⁰ *University of Michigan, Ann Arbor, United States, associated to ⁶⁷*
- ^a *Universidade Federal do Triângulo Mineiro (UFTM), Uberaba-MG, Brazil*
- ^b *Laboratoire Leprince-Ringuet, Palaiseau, France*
- ^c *P.N. Lebedev Physical Institute, Russian Academy of Science (LPI RAS), Moscow, Russia*
- ^d *Università di Bari, Bari, Italy*
- ^e *Università di Bologna, Bologna, Italy*
- ^f *Università di Cagliari, Cagliari, Italy*

- ^g *Università di Ferrara, Ferrara, Italy*
- ^h *Università di Genova, Genova, Italy*
- ⁱ *Università di Milano Bicocca, Milano, Italy*
- ^j *Università di Roma Tor Vergata, Roma, Italy*
- ^k *Università di Roma La Sapienza, Roma, Italy*
- ^l *AGH — University of Science and Technology, Faculty of Computer Science, Electronics and Telecommunications, Kraków, Poland*
- ^m *DS4DS, La Salle, Universitat Ramon Llull, Barcelona, Spain*
- ⁿ *Hanoi University of Science, Hanoi, Vietnam*
- ^o *Università di Padova, Padova, Italy*
- ^p *Università di Pisa, Pisa, Italy*
- ^q *Università degli Studi di Milano, Milano, Italy*
- ^r *Università di Urbino, Urbino, Italy*
- ^s *Università della Basilicata, Potenza, Italy*
- ^t *Scuola Normale Superiore, Pisa, Italy*
- ^u *Università di Modena e Reggio Emilia, Modena, Italy*
- ^v *Università di Siena, Siena, Italy*
- ^w *MSU — Iligan Institute of Technology (MSU-IIT), Iligan, Philippines*
- ^x *Novosibirsk State University, Novosibirsk, Russia*
- ^y *INFN Sezione di Trieste, Trieste, Italy*
- ^z *School of Physics and Information Technology, Shaanxi Normal University (SNNU), Xi'an, China*
- ^{aa} *Physics and Micro Electronic College, Hunan University, Changsha City, China*
- ^{ab} *Universidad Nacional Autonoma de Honduras, Tegucigalpa, Honduras*